Construction of second order accurate monotone and stable residual distributive schemes : the steady case.

Rémi Abgrall [1] and Mohamed Mezine
Mathématiques Appliquées de Bordeaux,
Université Bordeaux I,
351 cours de la Libération, 33 405 Talence Cedex
abgrall,mezine@math.u-bordeaux.fr

Keywords : Compressible flow solvers, Residual schemes, fluctuation splitting schemes, unstructured meshes, multidimensional up-winding.
AMS Subject Classification : 65C99, 65M60, 76N10

[1]institut Universitaire de France

Proposed running head : A stable, monotone, accurate residual distributive scheme for steady problems.

Rémi Abgrall
Mathématiques Appliquées de Bordeaux
351 Cours de la Libération
33 405 Talence Cedex
France
email : abgrall@math.u-bordeaux.fr
fax : +33 5 56 84 26 26

Send proof to Rémi Abgrall

Construction of second order accurate monotone and stable residual distributive schemes : the steady case.

Rémi Abgrall [†]and Mohamed Mezine
Mathématiques Appliquées de Bordeaux,
Université Bordeaux I,
351 cours de la Libération, 33 405 Talence Cedex
abgrall,mezine@math.u-bordeaux.fr

April 16, 2002

Abstract

We present the basic concept of residual distributive schemes for the Euler equations of fluid dynamics. Then, starting from a first order scalar scheme, stable in the L^∞ norm, we provide a systematic construction of distributive schemes able to handle general unstructured meshes, extending the work of Sidilkover. Then, by using the concept of simple waves, we show how to generalise this technic to symetrisable linear systems. A stability analysis is provided. We formaly extend this construction to the Euler equations using either the standard Roe scheme or the systeme N scheme of van der Weide and Deconinck. Several test cases are presented to validate our approach.

[†]institut Universitaire de France

Contents

1 Introduction

The numerical simulation of compressible flows is generaly done via generalisation of the one–dimensional Lax Wendroff scheme. It is well known that this scheme is stable in the energy norm, but does not have any stability property in the maximum norm. The simulation of flows with strong discontinuities can only be performed with schemes having properties in a maximum norm, because we want solutions exempt of numerical oscillations. This goal can be reached by modifications of the Lax Wendroff scheme, either by adding dissipative and fourth order terms monitored by complex ad-hoc, problem dependant, sensors, or via more automatic methods coming from the theory of scalar non linear schemes, see e.g. [16, 17] and the numerous references therein.

In each case, the approximation relies strongly on the structure of the one–dimensional problem. If the flow is represented by the values of the conservative unknowns at the mesh points, a consequence is, for example, that the accuracy of the solution degrades when going to multidimensional problems, especially and mainly with irregular meshes. The analysis via Taylor expansion and equivalent equation, that enables to study the formal accuracy of the scheme, is strictly valid only for one–dimensional problems. It can be extended to multidimensional problems only if the structure of the mesh allows special algebraic combinations resulting from the symetries of the mesh. If the flow is represented by the averaged values of the conservative unknowns on control volumes, there exists techniques to develop high order accurate schemes, for example the ENO or WENO schemes [2, 31, 18, 31, 19, 14]. In that case the analysis via the equivalent equation is different, but the main problem becomes a reconstruction problem, on variables that have to be chosen carefully [5]. The price to pay is a very large extension of the computational stencil. Even in that case, standard techniques uses Riemann solvers, so the fluxes are still computed in a one–dimensional spirit, resulting in large errors as analysed by van Leer [30]. Hence the overall quality of the scheme may be quite disapointing, in many cases.

In order tackle these two problems – compacity of the stencil, effective accuracy of the solution–, at least two classes of methods have emerged in the recent years, the Discontinuous Galerkin schemes (DG), and the Residual Distributive schemes (RD) or Fluctuation Splitting schemes. Though different in spirit, they have a common core at least in their "unstabilised" versions, the residual property. This property that we discuss below in the framework of RD schemes, allows to show the formal accuracy of the scheme on a very general mesh. The DG schemes use a discontinuous polynomial representation of the unknows that is a generalisation of what is done in finite volume schemes. The solution is updated via evaluation of fluxes, and the stabilisation mechanism is obtained by very similar techniques as in classical finite volume. The net effect of this is to loose the residual property.

On the contrary, the RD schemes use a pointwise representation of the solution, like in finite difference schemes. The unknowns are updated by evaluation the amount of residual sent to the vertices, and the stabilisation mechanism can be similar to artificial viscosity, as in the SUPG finite element method [20] or the Stream line diffusion method [22], or inspired by the nonlinear techniques of the so–called high resolution schemes [21, 17]. One can also take into account the genuinely multidimensional structure of the problem [27].

In this paper, we consider schemes of the RD class. Our goal is to propose a systematic construction of robust and high order schemes, on general meshes. This problem has received recently a lot of interest, one may quote the pionnering work of Roe, Sidilkover, Deconinck and their coworkers [12, 24, 27], and also more recently in [29, 3, 4, 11]. However, the solutions that are proposed in these contributions are not fully satisfactory, in particular, they may be not robust enough in some situations.

In this paper, we propose to reconsider the approach described in [24] for a very particular scheme, the scalar N scheme. Only steady problems are considered. This scheme has the special property that, on a triangular mesh, on each element, at least one residual vanishes, allowing very simple algebra. We show how to extend it to more general schemes where we do not need to assume a special structure of the underlying first order scheme. This approach, via a stability analysis using simple waves, enable to extend the method to linear symetrisable PDEs.

The format of the paper is the following. We first recall the formalism of Residual Distributive schemes, in particular we recall what is necessary to get second order accuracy. Then we analyse the scalar problems and show how to construct second order schemes. Going to system problem, we show some special properties of the Lax–Friedrichs scheme and the N scheme for symetrisable systems. These stability properties enable to justify formaly our construction. Several numerical tests, for linear and non linear PDEs demonstrate the qualities of our approach.

2 Generalities

Let us consider the equation of fluid mechanics

$$\begin{array}{ll} \dfrac{\partial W}{\partial t} + \text{ div } \mathbf{F}(W) = 0 & x \in \Omega, t > 0 \\ W(x,0) = W_0(x) & x \in \Omega, t = 0 \end{array} \tag{1}$$

supplemented by boundary conditions at the inflow, ouflow and solid boundaries. The vector of conservative variables W is defined by

$$W = (\rho, \rho\mathbf{u}, E)$$

where ρ is the density, $\mathbf{u}$ is the velocity, and $E = \rho\epsilon + \frac{1}{2}\rho\mathbf{u}^2$ is the total energy, ϵ being the internal energy per unit volume. The flux is defined by

$$\mathbf{F} = \begin{pmatrix} \rho\mathbf{u} \\ \rho\mathbf{u} \bigotimes \mathbf{u} + p\mathbf{Id} \\ \mathbf{u}(E+p) \end{pmatrix}.$$

Last, the pressure is defined by the perfect gas equation of state

$$p = (\gamma - 1)\Big(E - \frac{1}{2}\rho\mathbf{u}^2\Big).$$

In the sequel, the ratio of specific heats γ is assumed to be constant. In this paper, only steady problems are considered.

2.1 The residual distributive schemes

In order to approximate the steady problem,

$$\begin{array}{ll} \text{div } \mathbf{F}(W) = 0 & x \in \Omega \\ W(x,0) = W_0(x) & x \in \partial\Omega \\ \text{boundary conditions} & \end{array} \tag{2}$$

we consider a triangular mesh where the elements are denoted by $\{T_{j_t}\}_{jt=1,n_t}$, the vertices are denoted by $\{M_{is}\}_{is=1,ns}$. Strictly speaking, the vertices of T have to be indexed in the list $\{M_{is}\}_{is=1,ns}$, namely M_{i_1}, M_{i_2}, M_{i_3}. When there is no ambiguity, we denote them by i_1, i_2, i_3 or more simply $1, 2, 3$.

To approximate (2), we consider the following residual distributive scheme

$$|C_i| \frac{W_i^{n+1} - W_i^n}{\Delta t} + \sum_{T, M_i \in T} \Phi_i^T = 0 \tag{3}$$

where W_i^n is an approximation of $W(M_i, t_n)$ solution of (1), $|C_i|$ is the area of the dual control volume associated to M_i, Δt is the time step, and Φ_i^T stands for the residual sent by the element T to the vertex M_i. The residuals satisfy the following conservation relations

$$\sum_{j=1,3} \Phi_{i_j}^T = \int_T \text{div } \mathbf{F}^h dx := \Phi^T. \tag{4}$$

In (4), $\mathbf{F}^h$ is a continuous interpolation of the flux $\mathbf{F}$ that converges in L^1_{loc} to $\mathbf{F}$. In [6], we show that under the classical of the Lax Wendroff theorem, the limit solution of (3) are weak solutions of (1).

An example is given by finite volume type schemes on triangular meshes, see Figure 2 for the notations. If Q stands for the dissipation matrix, the numerical flux on the edge $[M_i, M_j]$ is

$$\begin{aligned} F(W_i, W_j, \vec{n}_{ij}) &= \frac{1}{2}\left(\mathbf{F}.\vec{n}^1_{ij}(W_j) + \mathbf{F}.\vec{n}^1_{ij}(W_i) - Q(W_i, W_j, \vec{n}^1_{ij}).(W_i - W_j)\right) \\ &+ \frac{1}{2}\left(\mathbf{F}.\vec{n}^2_{ij}(W_j) + \mathbf{F}.\vec{n}^2_{ij}(W_i) - Q(W_i, W_j, \vec{n}^2_{ij}).(W_i - W_j)\right). \end{aligned} \tag{5}$$

In (5), we have used the notation $\mathbf{F}.\vec{n}$ for $n_x\ F(W) + n_y\ G(W)$ where n_x and n_y are the componant of $\vec{n}$ and F, G the component of $\mathbf{F}$. Since the boundary of C_i is closed, the scheme is identical to the RD scheme (3) where we have set

$$\begin{aligned} \Phi_i^{T_1} &= \frac{1}{2}\left(\mathbf{F}.\vec{n}^1_{ij}(W_j) - \mathbf{F}.\vec{n}^1_{ij}(W_i) - Q(W_i, W_j, \vec{n}^1_{ij}).(W_i - W_j)\right) \\ &+ \frac{1}{2}\left(\mathbf{F}.\vec{n}^1_{ik}(W_k) - \mathbf{F}.\vec{n}^1_{ik}(W_i) - Q(W_i, W_k, \vec{n}^1_{ik}).(W_i - W_k)\right) \end{aligned} \tag{6}$$

and a similar expression for T_2. In (6), the indices j and k are the indices of the vertices of T_1 different of M_i. Finaly, we obtain

$$\sum_{M_i \in T_1} \Phi_i^{T_1} = \frac{1}{2} \sum_{M_i \in T_1} \mathbf{F}(W_i).\vec{n}_i$$

where $\vec{n}_j$ are the inward normal of the opposite face of T_1 to the vertex M_j. Here, the approximation $\mathbf{F}^h$ in (4) is the linear interpolation of $\mathbf{F}$ on T. Other examples, as the SUPG scheme, cast very naturaly in the same framework.

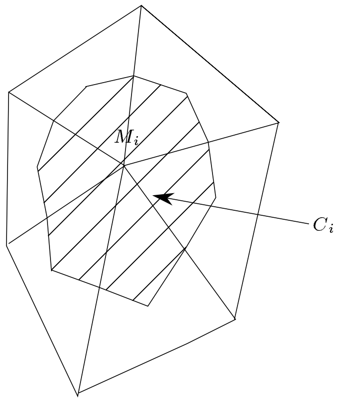

Figure 1: The dual control volume associated to M_i.

In the following, we develop a class of stable schemes able to approximate the solutions of (2). We start by recalling the concept or Linear Preserving schemes and its connection to accuracy considerations.

2.2 The residual property and the Linear Preserving condition

We recall a simple condition that garanties that the scheme is second order accurate *at steady state*.This condition has been introduced in [12], for example. It also implies that the scheme is at most first order during the transient phase.

At steady state, the scheme (3) satisfies

$$\text{whatever } M_i, \sum_{T, M_i \in T} \Phi_i^T = 0.$$

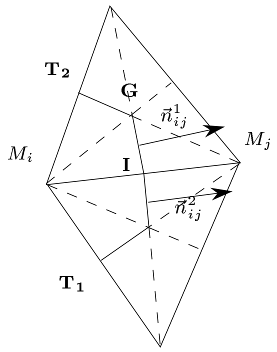

Figure 2: Geometry for the finite volume scheme. $\vec{n}^1_{ij}$ is orthogonal to $[G, I]$ with the same lenght. Same thing for $\vec{n}^2_{ij}$.

Hence, for any compactly supported test function $\varphi \in C^1(\mathbb{R}^2)^4$, we have

$$\sum_{M_i} \varphi_i \cdot \left(\sum_{T, M_i \in T} \Phi_i^T \right) = 0.$$

Setting $\varphi_G^T = \frac{\varphi_1 + \varphi_2 + \varphi_3}{3}$, we get, thanks to (4)

$$\sum_T \varphi_G^T \int_T \text{div } \mathbf{F}^h dxdy + \sum_T \sum_{M_i \in T} \left(\varphi_i - \varphi_G^T \right) \, . \, \Phi_i^T = 0,$$

that is, using the linearity of φ^h,

$$\int_\Omega \varphi^h \text{ div } \mathbf{F}^h dxdy + \sum_T \sum_{M_i \in T} \left(\varphi_i - \varphi_G^T \right) \, . \, \Phi_i^T = 0. \tag{7}$$

If the interpolation $\mathbf{F}^h$ is second order accurate, we note that

$$\int_\Omega \varphi^h \text{ div } \mathbf{F}^h dxdy = \mathcal{O}(h^2)$$

provided the mesh is regular, the solution is smooth and φ is a C^1 compactly supported test function. In this case,

$$\begin{aligned} \int_\Omega \varphi^h \text{ div } \mathbf{F}^h dxdy &= \int_\Omega \varphi^h \text{ div } \left(\mathbf{F}^h - \mathbf{F} \right) dxdy \\ &= \int_\Omega \left(\nabla \varphi^h, \left(\mathbf{F}^h - \mathbf{F} \right) \right) dxdy \\ &= \mathcal{O}(h^2). \end{aligned}$$

Here, h represents the maximum of the diameters of the triangles T. This shows that, under the second order accuracy assumption on the flux interpolation, we can recover the second order accuracy at steady state if the equivalent equation (7) of the scheme must satisfies

$$\sum_{M_i} \left(\varphi_i - \varphi_G^T \right) \cdot \left(\sum_{T, M_i \in T} \Phi_i^T \right) = \mathcal{O}(h^2) \tag{8}$$

when the residuals are computed by the value of a smooth solution of (1).

A way to get (8) is to have, for any smooth solution of (1), $\Phi_i^T(W) = \mathcal{O}(h^3)$ thanks to (7). This is quite clear from (7) because (i) the number of vertices of a bounded domain is $\mathcal{O}(h^{-2})$ for a regular mesh, (ii)

the equation (8) needs $(\varphi_i-\varphi_G)\Phi_i^T=\mathcal{O}(h^4)$ which is true because $\left|\left|\varphi_i-\varphi_G\right|\right|\leq\left|\left|\nabla\varphi^h\right|\right|_\infty h$ and $\left|\left|\nabla\varphi^h\right|\right|_\infty$ is known to be bounded for a smooth test function φ.

This condition is true for the SUPG schemes and the stream–line diffusion method, because the residual writes

$$\Phi_i^T=\beta_i^T\Phi^T$$

with β_i^T uniformly bounded.

Moreover, if W is a smooth solution of (1), we have $\Phi^T=\int_T \text{div }\mathbf{F}^h(W)dx=\mathcal{O}(h^3)$. In fact, we have

$$\begin{aligned}\int_T \text{div }\mathbf{F}^h(W)dx &= \int_T \text{div }\left(\mathbf{F}^h(W)-\mathbf{F}(W)\right)dx\\ &= \int_{\partial T}\left(\left(\mathbf{F}^h(W)-\mathbf{F}(W)\right),\vec{n}\right)dl\end{aligned}$$

Assuming that $\mathbf{F}^h$ is a second order approximation of $\mathbf{F}$, and since the lenght ∂T is $\mathcal{O}(h)$, we get

$$\Phi^T=\int_T \text{div }\mathbf{F}^h(W)dx=\mathcal{O}(h^3).$$

These arguments show clearly that *(i)* these scheme are second order accurate *only* for steady state, *(ii)* the approximation $\mathbf{F}^h$ of the flux must be second order accurate in some L^p norm. The condition

$$\Phi^T\rightarrow 0 \text{ implies } \Phi_i^T\rightarrow 0 \text{ whatever } i \text{ and uniformly}$$

is called the residual property or the linear preserving (LP) property. It is met by the SUPG like schemes. The unstabilized DG schemes possess a similar property.

2.3 Monotonicity preserving schemes

In this paragraph, we only consider scalar problems. We provide arguments for the system case below, as stated before, this is the main point of the paper.

In practice, all the known RD schemes can be written as

$$\Phi_i^T=\sum_{M_j\in T, M_i\neq M_i} c_{ij}^T(u_i-u_j). \tag{9}$$

By (3) and (9), we get

$$u_i^{n+1}=\sum_{M_j \text{neighbor of } M_i} d_{ij}u_j^n$$

with

$$\begin{aligned}d_{ii}&=1-\frac{\Delta t}{|C_i|}\sum_{T,M_i\in T}\sum_{M_j\in T,M_i\neq M_j}c_{ij}^T\\ d_{ij}&=\sum_{T,M_i,M_j\in T}\frac{\Delta t}{|C_i|}c_{ij}^T \qquad\qquad \text{if } M_i\neq M_j.\end{aligned}$$

The scheme is monotonicity preserving if $d_{ij}\geq 0$ (they sum up to unity). This is met if

$$\begin{aligned}&c_{ij}^T\geq 0 \qquad\qquad \text{for all } i,j\\ &\frac{\Delta t}{|C_i|}\sum_{T,M_i\in T}\sum_{M_j\in T,M_i\neq M_j}c_{ij}^T\leq 1.\end{aligned}$$

The condition $c_{ij}^T\geq 0$ is called the monotonicity condition. It is known that it is not possible to have a linear scheme (i.e. c_{ij}^T independant of the solution) that is both linear preserving and monotone [12]. The two conditions can be met if and only if the scheme is non linear. The construction of such schemes is the topic of the next section.

3 RD and LP discretisation of scalar equation

3.1 Construction

We consider the problem

$$\begin{array}{ll} \left(\vec{\lambda}, \nabla u\right) = 0 & x \in \Omega, t > 0 \\ u = g & \text{on } \Gamma_- \end{array} \tag{10}$$

where Γ_- is the inflow boundary of $\Gamma = \partial\Omega$. If the unknown u is piecewise linear interpolated, the total residual Φ^T is given by

$$\Phi^T = \sum_{j=1}^{3} k_j u_j$$

where

$$k_j = \frac{1}{2}\left(\vec{\lambda}, \vec{n_j}\right).$$

We notice that $\sum_{j=1}^{3} k_j = 0$. Here, and until the end of the paper, we have identified the vertices of T with the indices $j = 1, 2, 3$ because there is no ambiguity. Similarly, we drop the superscript T in $\Phi_i^T \equiv \Phi_i$.

We provide three examples of monotonicity preserving schemes. The first one is Rusanov' scheme,

$$\Phi_i^T = \frac{1}{3}\left(\Phi - \alpha \sum_{j \neq i}(u_i - u_j)\right) \tag{11}$$

with $\alpha \geq \max_i |k_i|$. We have clearly $\sum_j \Phi_j^T = \Phi$.

Another example is given by the N (narrow) scheme [12]. It writes

$$\Phi_i^T = k_i^+ (u_i - \widetilde{u}) \tag{12}$$

where $\widetilde{u}$ is obtained by recovering the conservation, i.e.

$$\widetilde{u} = \big(\sum_j k_j^-\big)^{-1}\big(\sum_j k_j^- u_j\big).$$

The scalar $n := \big(\sum_j k_j^-\Big)^{-1}$ is always defined unless $\vec{\lambda} = 0$[1]. This scheme can be considered as a conservative method of characteristics. It is monotone under a CFL like condition because

$$\Phi_i^T = \sum_j k_i^+ n k_j^- (u_i - u_j),$$

hence $c_{ij} = k_i^+ n k_j^- \geq 0$. A last example is provided by the classical upwind scheme. None of these scheme is linear preserving.

It is important to construct schemes that preserves both the monotonicity and the linear preserving properties. Thanks to Godunov's theorem, these schemes are non linear. Several constructions are possible. One may quote the PSI scheme of Struijs [10], Sidilkover's construction of the same scheme [25]. Another method is the hybridation technique of [3, 28] which consists in blending a first order monotone scheme (residual $\Phi_i^{(1)}$) and a second order LP scheme (residual $\Phi_i^{(2)}$),

$$\Phi_i = \ell\Phi_i^{(1)} + (1-\ell)\Phi_i^{(2)}.$$

[1] Since for any i, $\Phi_i \to 0$ uniformly if $\vec{\lambda} \to 0$, there is no definition problem in the case $\vec{\lambda} = 0$.

The solution provided by the blending technique is not the ultimate one. Deconinck et al B scheme [28] is not monotonicity preserving, even though it is not easy to exhibit an oscilatory counter–example. The solution of [3] is also not a final one because the two schemes must have some compatibility relations otherwise the blended scheme might indeed reduce to the first order one, i.e. $\ell \simeq 1$. A good example is given by the blending of the N scheme and the LDA scheme, which reduces for scalar problems to the PSI scheme, once more. The LDA scheme is defined by

$$\Phi_i = -nk_i^+\Phi.$$

An example where $\ell \simeq 1$ much too often is the blending of the Lax Wendroff scheme

$$\Phi_i = \frac{\Phi}{3} - \alpha\Delta t k_i \Phi$$

for some positive α and the N scheme. The problem here is that the N scheme is upwind, while the Lax Wendroff is not, so that we might have $\Phi_i = 0$ for the N scheme and $\Phi_i \neq 0$ for the Lax Wendroff scheme. Since ℓ is defined by a relation of the type

$$\ell = \max_{i=1,3} \varphi(r_i)$$

where r_i is the ratio of the second order residual versus the first order one, we have in general $\ell = 1$, see [3] for details. In some cases, the LP condition is not so clear, for example in the example of the blending of the Rusanov and the Lax Wendroff scheme is monotonicity preserving by construction but its LP property is not clear.

This is why we have tried to develop another construction, partially inspired from Sidilkover, but in our opinion more powerfull since non triangular elements can be considered. The construction basicaly relies on the existence of an first order monotone scheme, and provide a systematic way of defining a LP monotone scheme.

We start from a first order monotonicity preserving scheme,

$$\Phi_i = \sum_j c_{ij}(u_i - u_j), \qquad c_{ij} \geq 0.$$

To simplify the notations, we present the technique on triangular elements, but the extension to more gereral elements is obvious.

As Sidilkover, we want to construct a residual Φ_i^* such that *(i)* The scheme defined by Φ_i^* is monotonicity preserving, *(ii)* The scheme is conservative, i.e. $\sum\limits_j \Phi_j^* = \sum\limits_j \Phi_j = \Phi$, *(iii)* The scheme is LP, more precisely, we want $\beta_i := \frac{\Phi_i^*}{\Phi}$ bounded.

The first condition writes

$$1 - \mu_i = \frac{\Phi_i^*}{\Phi_i} \geq 0,$$

i.e. $\mu_i \leq 1$. The second condition writes

$$\sum_j \mu_j \Phi_j = 0.$$

Before going further, let us examine the L^∞ stability condition. The stability condition of the first order scheme is

$$\Delta t \max_T \max_{j=1,3} \frac{\sum\limits_k c_{ik}}{|T|} \leq 1$$

i.e.

$$\Delta t \leq \Delta t^{(1)} := \frac{1}{\max_T \max_i \frac{\sum\limits_k c_{ik}}{|T|}}. \tag{13}$$

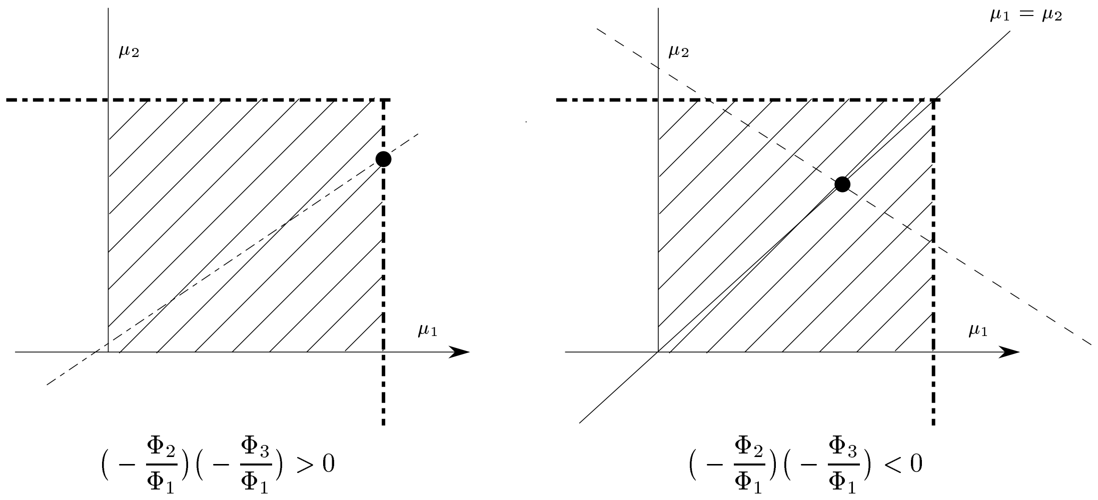

Figure 3: Some possible configurations in the solution of (17)

Thus, the natural stability condition of the new scheme is

$$\Delta t \leq \Delta t^{(2)} := \frac{1}{\max_T \max_i \dfrac{(1-\mu_i)\sum_k c_{ik}}{|T|}}. \tag{14}$$

Since $\mu_i \leq 1$, it is clear that $\Delta t^{(2)} \leq \Delta t^{(1)}$. If we want that the maximum time step of the first order scheme is of the order of that of the new scheme, it is better that $1-\mu_i$ is not too large, that is μ_i is not too large. For this reason, we ask

$$0 \leq \mu_i \leq 1. \tag{15}$$

Using the previous notations, the LP condition is

$$\beta_i = (1-\mu_i)\frac{\Phi_i^*}{\Phi} \text{ bounded.}$$

For that reason, we demand $\mu_i = 1$ as often as possible.

To summarise, the problem is : find $\{\mu_j\}_{j=1,N} \in [0,1]^N$ such that

$$\begin{aligned} &\sum_{j=1}^N \mu_j \Phi_j = 0 \\ &\{\mu_j\}_{j=1,N} \in [0,1]^N \text{ and on the boundary of }]-\infty,1]^N \end{aligned} \tag{16}$$

Assume $N=3$ for simplicity. The problem is

$$\Phi_1\mu_1 + \Phi_2\mu_2 + \Phi_3\mu_3 = 0. \tag{17}$$

with

$$0 \leq \mu_i \leq 1. \tag{18}$$

We are looking for solutions where $\mu_j = 1$ (i.e $\Phi_j^* = 0$) as often as possible, and for which the new scheme depends continuously on the parameters.

We may assume $\Phi_1 \neq 0$. The equation (17) becomes

$$\mu_1 = \mu_2\big(-\frac{\Phi_2}{\Phi_1}\big) + \mu_3\big(-\frac{\Phi_3}{\Phi_1}\big)$$

The solutions we are seeking are those for which $\mu_1 = 1$ as often as possible, without violating the monotonicity condition.

1. If $\big(-\frac{\Phi_2}{\Phi_1}\big)\big(-\frac{\Phi_3}{\Phi_1}\big) > 0$, see Figure 3. The line defined by

$$1 = \mu_2\big(-\frac{\Phi_2}{\Phi_1}\big) + \mu_3\big(-\frac{\Phi_3}{\Phi_1}\big)$$

has either an empty intersection with $[0,1]^2$, or has two intersection points. For symetry reasons, we assume $\mu_1 = \mu_2 = \mu$, hence

$$\mu = -\frac{\Phi_1}{\Phi_2 + \Phi_3}.$$

(a) If $\mu < 0$, then we take $\mu_2 = \mu_3 = \mu_1 = 0$ and then $\Phi_i^* = \Phi_i$, $i = 1, 3$. We notice that

$$\frac{\Phi_1}{\Phi} = \frac{1}{1 + \dfrac{\Phi_2 + \Phi_3}{\Phi_1}} \in [0,1]$$
$$\frac{\Phi_2}{\Phi} = \frac{1}{1 + \dfrac{\Phi_1 + \Phi_3}{\Phi_3}} \in [0,1]$$
$$\frac{\Phi_3}{\Phi} = \frac{1}{1 + \dfrac{\Phi_2 + \Phi_1}{\Phi_3}} \in [0,1]$$

The first claim is true because $\dfrac{\Phi_1}{\Phi_2 + \Phi_3} > 0$. The second one is also true because Φ_2 and Φ_3 beeing of the same sign and $\mu > 0$ implies that Φ_1, Φ_2 and Φ_3 have the same sign and then $\dfrac{\Phi_1 + \Phi_3}{\Phi_3} > 0$. The third claim is true for the same reason. This shows that β_i is bounded in that case.

(b) If $0 < \mu < 1$ then

$$\Phi_1^* = 0$$
$$\Phi_2^* = \frac{\Phi_2}{\Phi_2 + \Phi_3}\Phi$$
$$\Phi_3^* = \frac{\Phi_3}{\Phi_2 + \Phi_3}\Phi.$$

The coefficients β_i are bounded because $0 \le \dfrac{\Phi_2}{\Phi_2 + \Phi_3} \le 1$.

(c) If $\mu > 1$, then

$$\Phi_1^* = \Phi$$
$$\Phi_2^* = 0$$
$$\Phi_3^* = 0,$$

the β_is are clearly bounded.

2. If $\big(-\frac{\Phi_2}{\Phi_1}\big)\big(-\frac{\Phi_3}{\Phi_1}\big) < 0$, see Figure 3, the line

$$1 = \mu_2\big(-\frac{\Phi_2}{\Phi_1}\big) + \mu_3\big(-\frac{\Phi_3}{\Phi_1}\big)$$

cuts the boundary $0 \le \mu_1 \le 1$ or $0 \le \mu_2 \le 1$ in at most one point. The intersection points are

$$\mu_2 = 1, \mu_3 = -\frac{\Phi_2 + \Phi_1}{\Phi_3} \text{ and } \mu_3 = 1, \mu_2 = -\frac{\Phi_3 + \Phi_1}{\Phi_2},$$

see Figure 3

(a) If $\mu_2 = 1, \mu_3 = -\dfrac{\Phi_2 + \Phi_1}{\Phi_3} < 0$, we set

$$\begin{array}{l} \Phi_1^* = \Phi_1 + \Phi_2 \\ \Phi_2^* = 0 \\ \Phi_3^* = \Phi_3, \end{array}$$

once more β_i is bounded because

$$\frac{\Phi_3^*}{\Phi} = \frac{1}{\dfrac{\Phi_1 + \Phi_2}{\Phi_3} + 1} \in [0, 1]$$

and $\dfrac{\Phi_1}{\Phi}$.

(b) If $\mu_2 = 1, \mu_3 = -\dfrac{\Phi_2 + \Phi_1}{\Phi_3} \in [0, 1]$, we set

$$\begin{array}{l} \Phi_1^* = 0 \\ \Phi_2^* = 0 \\ \Phi_3^* = \Phi \end{array}$$

(c) If $\mu_3 = 1, \mu_2 = -\dfrac{\Phi_3 + \Phi_1}{\Phi_2} \in [0, 1]$, we set

$$\begin{array}{l} \Phi_1^* = 0 \\ \Phi_2^* = \Phi \\ \Phi_3^* = 0 \end{array}$$

(d) If $\mu_3 = 1, \mu_2 = -\dfrac{\Phi_3 + \Phi_1}{\Phi_1} < 0$, we set

$$\begin{array}{l} \Phi_1^* = \Phi_1 + \Phi_3 \\ \Phi_2^* = \Phi_2 \\ \Phi_3^* = 0, \end{array}$$

for which the β_is are bounded.

The scheme defined as above is continuous : If one re–examine the coefficients β_i, we see that our solution satisfy either $0 \leq \beta_i < 1$ or $\beta_1 = 0$ and $\beta_2, \beta_3 \in [0, 1]$ with a continous dependancy.

In this construction, the node $i = 1$ plays a special role, so the scheme is numbering dependant. This is why a better solution is to average the three solutions obtained by making the vertices $i = 1$, then $i = 2$ then $i = 3$ play a pivot role. This scheme is now continous and independant of the numebring of the mesh points.

A simplier solution is to make the construction on the pivot index i_0 the index for which $|\Phi_j|$ is maximum. This is the solution we use in all the numerical illustration. The previous solutions gives results that undistinguishable from those obtained by this one.

3.2 Numerical illustrations

We apply the above construction to

$$\begin{array}{ll} \dfrac{1}{2}\dfrac{\partial u^2}{\partial x} + \dfrac{\partial u}{\partial y} = 0 & (x, y) \in [0, 1]^2 \\ u(x, 0) = 1.5 - x & u(0, y) = 1.5 \\ u(1, y) = 0.5 & \end{array} \tag{19}$$

The PDE (19) is non linear. The link between (19) to a linear PDE is obtained via a conservative linearisation [10], i.e. we determine for each triangle $\bar{u}$ such that

$$\int_T \left(\frac{1}{2}\frac{\partial u^2}{\partial x} + \frac{\partial u}{\partial y}\right) dxdy = \bar{u} \int_T \frac{\partial u}{\partial x} dxdy + \int_T \frac{\partial u}{\partial y} dxdy. \tag{20}$$

In the left hand side of (20), u is piecewise linearly interpolated. The obvious solution is $\bar{u} = \frac{1}{3} \sum_{j=1,3} u_{i_j}$.

The total residual is distributed

$$\Phi = \bar{u} \int_T \frac{\partial u}{\partial x} dxdy + \int_T \frac{\partial u}{\partial y} dxdy$$

by mean of any of the three schemes described above, Rusanov' scheme, the N scheme and the first order upwind scheme. We will consider two versions of the upwind scheme. One uses the classical 1D Murman–Roe scheme adapted to (19), rewritten in the distribution framework, the other one is constructed from the linearisation (20). For comparison purposes, we display the mesh on Figure 4 and the solution obtained by a standard second order ENO scheme on unstructured meshes.

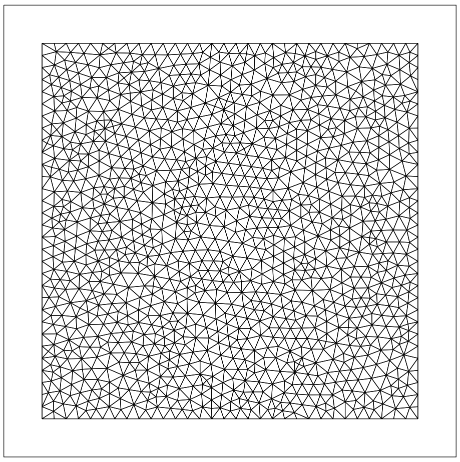

Figure 4: Mesh

The scheme constructed from the Rusanov' scheme (resp. the N scheme, the 1D upwind scheme and the 2D Roe average) is denoted by L–Rusanov[2] (resp. Psi, L–Roe–1D and L–Roe–2D). The solutions are plotted on Figures (5) and(6).

Then we plot cross–sections in the discontinuity in Figure (7). On Figure (8), we have displayed cross–section plots in the fan.

We see that the quality of the results is *always* better for the second order distributive schemes than for the second order ENO scheme. This is a consequence of the residual property shared by these schemes. Among them, there is a hierarchy : the PSI scheme is the best, the results for the upwind scheme are almost similar, followed by those for L-Rusanov. For the latter scheme, the results seem a bit wigly in the fan. This is not a stability problem, since the results are converged. We believe that since Rusanov' scheme is very dissipative, the limitation mechanism that we propose is probably too overcompressive.

[2]L– for limited

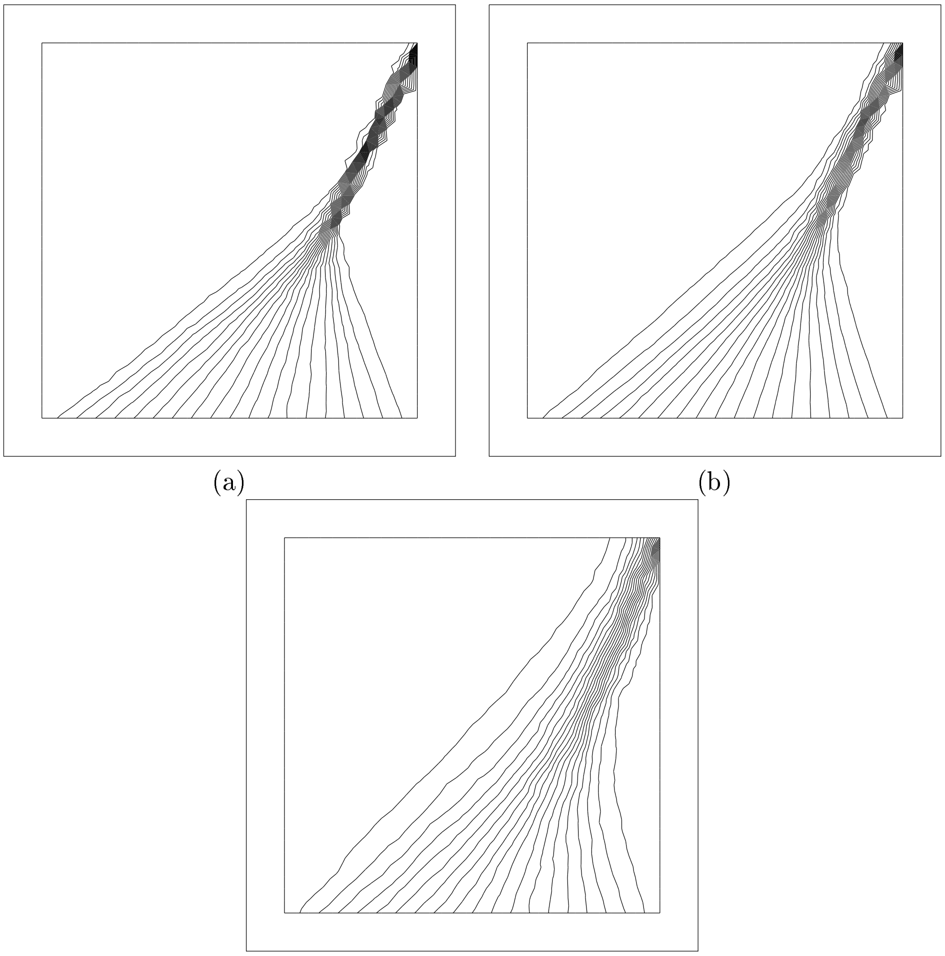

(a) (b)

(c)

Figure 5: (a) : N scheme, (b) Upwind scheme, (c) Rusanov's scheme

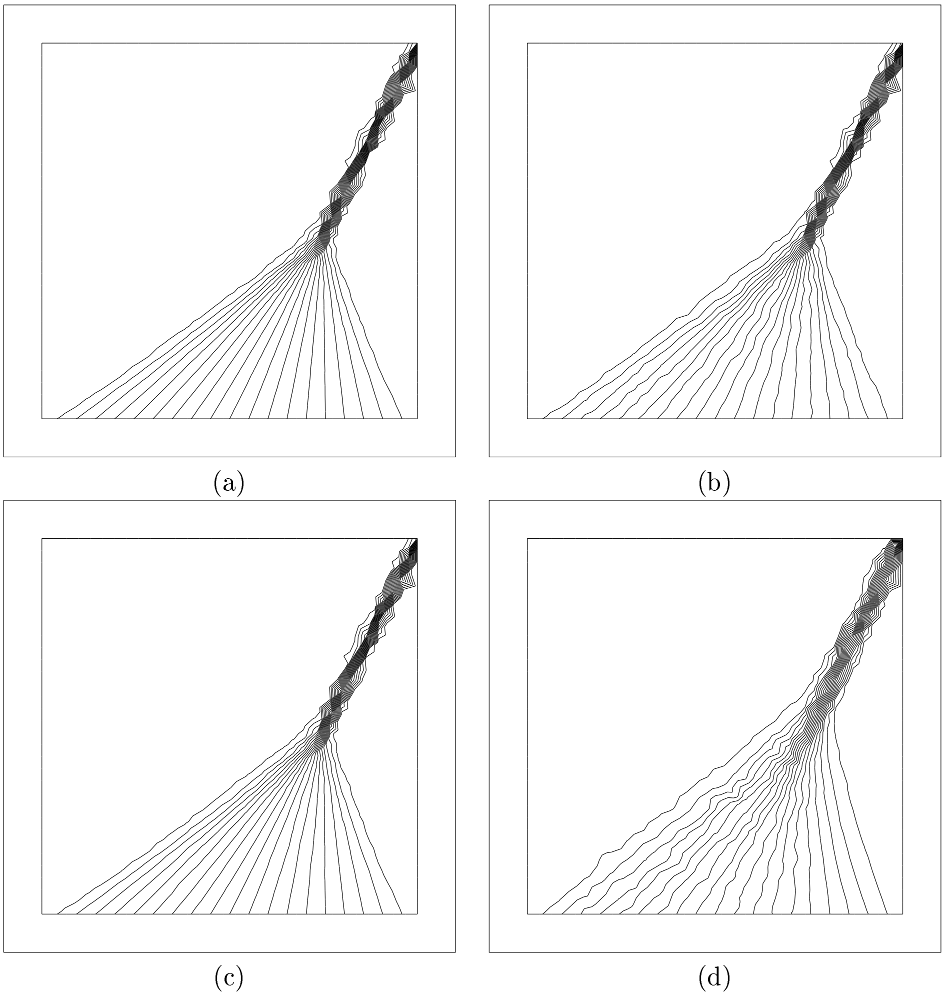

Figure 6: (a) Psi, (b) : L–Rusanov , (c) L–Upwind, (d) Second order ENO scheme

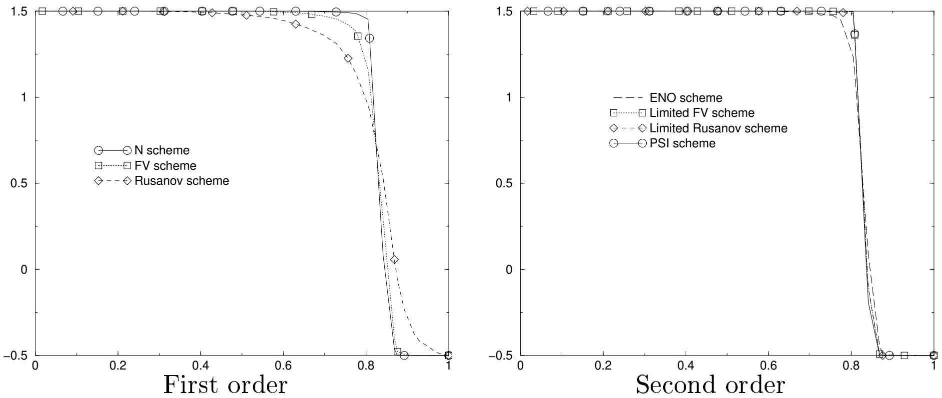

Figure 7: Cross–sections in the shock

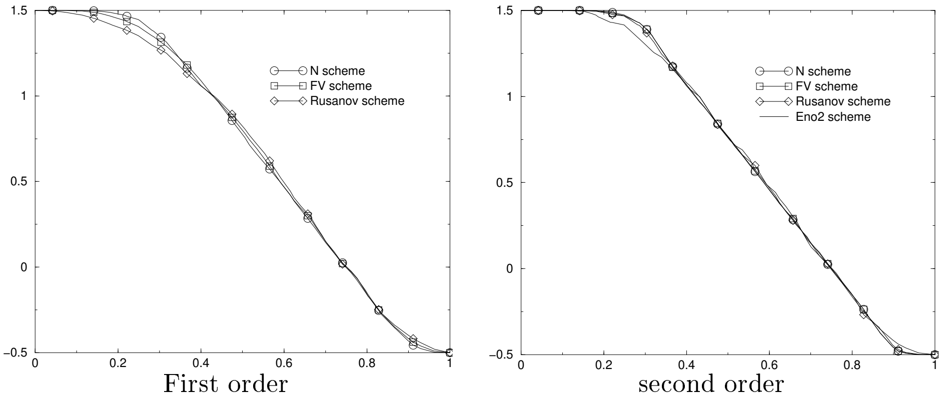

Figure 8: Cross–section in the fan

4 Going to linear hyperbolic systems

The main difficulty to step from scalar to systems PDEs of the type

$$A\frac{\partial U}{\partial x} + B\frac{\partial U}{\partial y} = 0 \quad \text{Boundary conditions} \tag{21}$$

is that, in general, the two Jacobian matrices A and B do not commute. The consequence is that there exists no basis of common eigenvectors to the matrices A and B. However, the analysis of the Cauchy problem

$$\frac{\partial U}{\partial t} + A\frac{\partial U}{\partial x} + B\frac{\partial U}{\partial y} = 0 \quad \text{Boundary and initial conditions} \tag{22}$$

when the initial and boundary conditions are piecewise smooth and the Jacobian matrices are symmetric show that the solution is piecewise smooth, without high frequency oscillations at the discontinuities. See for example [1, 15] in the case of Riemann data.

Unfortunately, the systems (21-22) are well posed only in L^2 or in Hilbert spaces which use in the analysis of a numerical scheme seems very complex [8, 9]. However, the analysis of [1] is very easy to extend to P^k initial data. It seems legitimate, and all the numerical experiments show this, to seek for stability criterion that have a L^∞ flavor in order to control the oscillations of an approximating scheme for (21).

In the following, we first recall some particular distributive schemes. We show some of their properties, in particular when applied to simple waves. These properties justify, in our opinion, the heuristic arguments we use to construct stable LP schemes.

4.1 Some RD schemes for (21)

If one interpolate U linearly in each triangle, the total residual Φ associated to (21) writes

$$\Phi = \int_T \left(A\frac{\partial U}{\partial x} + B\frac{\partial U}{\partial y}\right) = \sum_{j=1,3} K_j U_j \tag{23}$$

where the conservative variables at the vertices of T are denoted by U_j and the matrices K_j are

$$K_j = n_x^j A + n_y^j B$$

where n_x^j and n_y^j represent the components of $\vec{n}_j$, the inward unit normal vector opposite to M_j, i.e.

$$\vec{n}_j = 2|T|\nabla\Lambda_j$$

if Λ_i is the barycentric coordinate at M_i. Sometimes, we denote K_n the matrix

$$K_n = n_x A + n_y B$$

where $\vec{n} = (n_x, n_y)$.

Thanks to these definitions, the Rusanov scheme is

$$\Phi_i = \frac{1}{3}\Big(\Phi - \alpha \sum_j (U_i - U_j)\Big) \tag{24}$$

with $\alpha \geq \max_j ||K_j||$.

The system N scheme [29] writes

$$\Phi_i = K_i^+ \big(U_i - \widetilde{U}\big) \tag{25}$$

where $\widetilde{U}$ is computed to recover the conservation property :

$$\Big(\sum_j K_j^-\Big)\widetilde{U} = \sum_j K_j^- U_j.$$

The matrix $\sum\limits_j K_j^-$ is invertible as soon as A and B have no common eigenvectors [3]. When there exist common eigenvectors, $\sum\limits_j K_j^-$ may be no longer invertible but the matrices NK_j^- have a meaning, see [3] for details. In each case, the scheme (25) is well defined [3].

Let us denote $(\mathbf{x}, \mathbf{y})$ the dot product of the vectors $\mathbf{x}$ and $\mathbf{y}$.

In each case, we have $\sum\limits_j \Phi_j = K_j U_j$. We remark [4] that the production of energy writes

$$\mathcal{T}(U_1, U_2, U_3) = \sum_j \,(U_j, \Phi_j)$$

where

$$\mathcal{T}(U_1, U_2, U_3) = \frac{1}{2}\sum_j \,(U_j, K_j U_j) - \mathcal{Q}(U_1, U_2, U_3)$$

with $\frac{1}{2}\sum\limits_j \,(U_j, K_j U_j)$ is a consistant approximation of

$$\frac{1}{2}\int_T \text{div }\ (U, \mathbf{F})\, dx$$

and $\mathcal{Q}$ is a negative quadratic form, in the two cases considered above. This show that the three schemes are dissipative.

Last, we notice that the scheme (3) can be rewritten as

$$U_i^{n+1} = \sum_{T, M_j \in T} \frac{|T|}{|C_i|} \widetilde{U}_i^{n+1} \tag{26}$$

with

$$\widetilde{U}_i^{n+1} = U_i^n - \frac{\Delta t}{|T|}\Phi_i^T. \tag{27}$$

This enable to localise the analysis on each of the triangles of the mesh.

4.2 Stability analysis by simple waves

We call simple wave a solution of the type

$$U(x) = \mathbf{C} + \beta\,(\vec{n}, \mathbf{x})\,\mathbf{r}$$

where $\mathbf{C}$ is a constant vector, $\mathbf{x}$ is any point, $\mathbf{r}$ is a normalised eigenvector of the matrix $K_{\vec{n}}$. The function U is linear in T, its nodal values are still denoted by U_j. Last, we still denote $\varphi_j = (U_j, \mathbf{r})$, i.e. $U_j = \varphi_j \mathbf{r} + \mathbf{C}$.

We notice that

$$A\frac{\partial U}{\partial x} + B\frac{\partial U}{\partial y} = K_{\vec{n}}\mathbf{r} = \lambda(\mathbf{r})\mathbf{r}$$

where $\lambda(\mathbf{r})$ is the eigenvalue associated to $\mathbf{r}$, hence Φ is proportional to $\mathbf{r}$.

Our aim is to justify the experimental fact that the Rusanov', N and finite volume schemes are monotonicity preserving, i.e., there is no creation of numerical oscillation.

4.2.1 Wave decomposition

The first remark is that, locally in a triangle, U^n is th sum of simple waves. In fact, in T

$$U(\mathbf{x}) = \sum_j U_j \Lambda_j(\mathbf{x})$$

with

$$\Lambda_j(\mathbf{x}) = \frac{(\vec{n}_i, \mathbf{x})}{2|T|}.$$

Calling $\{\mathbf{r}_\xi\}$ an orthogonal basis of eigenvectors of $K_{\vec{n}}$, we may write

$$U(\mathbf{x}) = \frac{1}{2|T|}\sum_{j=1,3}\sum_{\xi}\big(\,(U_j, \mathbf{r}_\xi)\,\big)\big(\,(\vec{n}_i, \mathbf{x})\,\big)\mathbf{r}_\xi. \tag{28}$$

This shows that a piecewise linear U is a sum of the simple waves.

The decomposition is not unique. Depending on the scheme, we might need "adapted" wave decomposition to prove our claim, but the central idea is contained in (28).

4.2.2 Case of Rusanov' scheme

In this case, we have

$$\Phi_i = \frac{1}{3}\big(\Phi - \alpha\sum_j (U_i - U_j)\big)$$

with U_j proportional to $\mathbf{r}$. Hence, Φ_i is proportional to $\mathbf{r}$. This shows that

$$\Phi_i = (\Phi_i, \mathbf{r})\,\mathbf{r}$$

with

$$(\Phi_i, \mathbf{r}) = \sum_j \frac{1}{3}\left(\Big((K_j - \alpha\mathbf{Id})\mathbf{r}\Big), \mathbf{r}\right)(\varphi_i - \varphi_j)$$

and, by definition of α,

$$c_{ij}^R := \frac{1}{3}\left(\Big((K_j - \alpha\mathbf{Id})\mathbf{r}\Big), \mathbf{r}\right) \geq 0.$$

We consider then the iterative scheme

$$\widetilde{U}_j^{n+1} = U_j^n - \frac{\Delta t}{|C_j|}\sum_{T, M_j \in T}\Phi_j.$$

It writes for a simple wave

$$\widetilde{U}_j^{n+1}=\left(\varphi_i-\frac{\Delta t}{|C_i|}\sum_{T,M_i\in T}\sum_{M_j\in T}c_{ij}^R(\varphi_i-\varphi_j)\right)\mathbf{r}. \tag{29}$$

This shows that the simple wave evolves proportionaly to $\mathbf{r}$, and $||\widetilde{U}_i^{n+1}||\leq \max_{M_j\in T}||U_j^n||$ under a CFL type condition[3], and a single time step. Then, thanks to (26),

$$||U_i^{n+1}||\leq \max_{M_j \text{ neighbor of } M_i}||U_j^n||.$$

This does *not* show that if U^n is globaly a simple wave, so will be U^{n+1}. But it shows that the profile of the solution remains monotone.

We see that in general, $\widetilde{U}_j^{n+1}$ is a linear combination of terms like (29), that are averaged according to (26). This is a strong indication that there is no creation of spurious oscillations.

Remark 4.1. *This analysis is done only for one time step. We are not able to provide any property on the behavior of $||U||$ for example. This is not very surprising because the natural norm here is the L^∞ norm. It is known that the problem*

$$\begin{array}{l}\dfrac{\partial U}{\partial t}+A\dfrac{\partial U}{\partial x}+B\dfrac{\partial U}{\partial y}=0\\ \textit{Initial conditions}\end{array}$$

is ill–posed in L^∞ [8]. The pertinent norms, described in [9], seem difficult to handle in practice.

4.2.3 Case of the system N scheme

The system N scheme write

$$\mathbf{\Phi}_i=\mathbf{K}_i^+\sum_j \mathbf{N}\mathbf{K}_j^-(U_i-U_j) \tag{30}$$

with $\mathbf{N}=\left(\sum_j \mathbf{K}_j^-\right)^{-1}$. We start by reducing the problem to the case where $N=-\mathrm{Id}$ thanks to a (local) change of variable.

We write

$$\begin{array}{rcl}\mathbf{K}_i^+\sum_j\mathbf{N}\mathbf{K}_j^-(U_i-U_j)&=&\mathbf{K}_i^+\mathbf{M}\sum_j\mathbf{K}_j^-(U_j-U_i)\\ &=&\mathbf{M}^{1/2}\left(\mathbf{M}^{-1/2}\mathbf{K}_i^+\mathbf{M}^{1/2}\right)\sum_j\left(\mathbf{M}^{1/2}\mathbf{K}_j^-\mathbf{M}^{1/2}\right)(\mathbf{M}^{-1/2}U_j-\mathbf{M}^{-1/2}U_i)\end{array}$$

with $\mathbf{M}=-\mathbf{N}>0$.

We make the change of variable $\widetilde{\mathbf{K}}_j=\mathbf{M}^{1/2}K_j\mathbf{M}^{1/2}$, $\widetilde{\mathcal{K}}_j=\mathbf{M}^{-1/2}K_j\mathbf{M}^{1/2}$, and $\mathbf{V}=\mathbf{M}^{-1/2}U$. We get

$$\widetilde{\mathbf{K}}_j^{\pm}=\mathbf{M}^{1/2}K_j^{\pm}\mathbf{M}^{1/2} \text{ and } \widetilde{\mathcal{K}}_j^{\pm}=\mathbf{M}^{-1/2}K_j^{\pm}\mathbf{M}^{1/2}$$

because the matrices are symetric. Hence, the residual writes

$$\mathbf{\Phi}_i=\mathbf{M}^{1/2}\sum_j\widetilde{\mathcal{K}}_i^+\widetilde{\mathbf{K}}_j^-(\mathbf{V}_j-\mathbf{V}_i),$$

and the scheme (30) becomes

$$\mathbf{V}_i^{n+1}=\mathbf{V}_i^n-\frac{\Delta t}{|T|}\widetilde{\mathcal{K}}_i^+\left(\sum_j\widetilde{\mathbf{K}}_j^-(\mathbf{V}_j-\mathbf{V}_i)\right)=\mathbf{V}_i^n-\frac{\Delta t}{|T|}\widetilde{\mathcal{K}}_i^+\left[\left(\sum_j\widetilde{\mathbf{K}}_j^-\mathbf{V}_j\right)+\mathbf{V}_i\right] \tag{31}$$

[3] à préciser

for which $\mathbf{N}=-\mathrm{Id}$ and the matrices $\widetilde{\mathbf{K}}_i$, $\widetilde{\mathcal{K}}_i$ are symetric. This is why, in the following, we assume that $\mathbf{N}=-\mathrm{Id}$. From now on, we write with the form (31) of the scheme, even though, strictly speaking, it is not any longer the N scheme. As we have seen before, it is important to write the vector

$$\left(\sum_j \widetilde{\mathbf{K}}_j^- \mathbf{V}_j\right) + \mathbf{V}_i$$

as a sum of simple waves. The matrix $\widetilde{\mathcal{K}}_i$ plays the role of a combination of projectors.

We consider $\mathbf{V}$, the linear interpolation of $\mathbf{V}_j$ on T. We see that

$$\mathbf{V}(x) = \mathbf{V}_0 + \sum_{j=1}^{3} \frac{(\vec{n}_j, x)}{2|T|}\,\mathbf{V}_j$$

where $\vec{n}_i$ is the inward normal unit opposite to the node i of T and $\mathbf{V}_0$ is a constant vector.

The second step is to rewrite this egality with the right (resp. left) eigenvectors $\mathbf{r}_l^j$ (resp. $\underline{\ell}_l^j$) of $\mathbf{K}_j$ (with $\underline{\ell}_l^k(\mathbf{r}_l^i)=\delta_i^k$),

$$\mathbf{V}(x) = \mathbf{V}_0 + \sum_{j=1}^{3}\sum_{l=1}^{4} \frac{(\vec{n}_j, x)}{2|T|}\underline{\ell}_l^j(\mathbf{V}_j)\mathbf{r}_l^j$$

The last step is to introduce a point M_i' on the side opposite to the vertex i, see Figure 9, and to rewrite

$$\mathbf{V}(x) = \mathbf{V}_0' + \sum_{j=1}^{3}\sum_{l=1}^{4} \frac{\left(\vec{n}_j, \overrightarrow{M_j'\mathbf{x}}\right)}{2|T|}\underline{\ell}_l^j(\mathbf{V}_j)\mathbf{r}_l^j := \mathbf{V}_0 + \sum_{j=1}^{3}\sum_{l=1}^{4} \underline{\ell}_l^j(\mathbf{V}_j)\varphi_l^j(\mathbf{x})\mathbf{r}_l^j, \tag{32}$$

i.e., as a sum of simple waves.

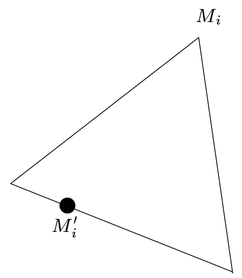

Figure 9: Definition of M_i' in (32).

We notice, thanks to the definition of M_i',

$$\begin{aligned}\varphi_j^l(M_i)\mathbf{r}_l^j &= 0\\ \varphi_j^l(M_k)\mathbf{r}_l^j &= 0\\ \varphi_j^l(M_j)\mathbf{r}_l^j &\neq 0\end{aligned}$$

Since the N scheme is linear, it is enough to evaluate the N scheme on each of the simple waves. Let us consider the wave that vanishes for $j=2$ and 3. It is proportional to $\mathbf{r}_l^1$:

$$\mathbf{V}_i = \alpha\varphi_l^1(M_i)\mathbf{r}_l^1.$$

We may assume that $\alpha=1$. We have

$$\mathbf{V}_i^{n+1} = \varphi_l^1(M_i)\mathbf{r}_l^1 - \frac{\Delta t}{|T|}\widetilde{\mathcal{K}}_i^+\left(\varphi_l^1(M_i)\mathbf{r}_l^1 + \widetilde{\mathbf{V}}\right)$$

with

$$\widetilde{\mathbf{V}} = \varphi_l^1(M_1)\,\mathbf{K}_1^-\mathbf{r}_l^1 = \lambda_l^-\varphi_l^1(M_1)\mathbf{r}_1^j.$$

Hence,

$$\varphi_l^1(M_i)\mathbf{r}_l^1 + \widetilde{\mathbf{V}} = \left(\varphi_l^1(M_i) + \lambda_l^-\varphi_l^1(M_1)\right)\mathbf{r}_l^j$$

where λ_l is the eigenvalue of $\mathbf{K}_1$ associated to $\mathbf{r}_l^1$, and then

$$\mathbf{V}_i^{n+1} = \varphi_l^1(M_i)\mathbf{r}_l^1 - \frac{\Delta t}{|T|}\left(\varphi_l^1(M_i) + \lambda_l^-\varphi_l^1(M_1)\right)\widetilde{\mathcal{K}}_i^+\mathbf{r}_l^1.$$

Let us introduce $\mathbf{\Upsilon}_i^p$ the left eigenvector of $\widetilde{\mathcal{K}}_i$ and μ_i^p the corresponding eigenvalue. We have

$$\mathbf{\Upsilon}_i^p(\mathbf{V}_i^{n+1}) = \left\{\varphi_l^1(M_i) - \frac{\Delta t}{|T|}\left[\left(\mu_i^p\right)^+\left(\varphi_l^1(M_i) + \lambda_l^-\varphi_l^1(M_1)\right)\right]\right\}\mathbf{\Upsilon}_i^p(\mathbf{r}_l^1),$$

that is

$$\mathbf{\Upsilon}_i^p(\mathbf{V}_i^{n+1}) = \left\{\left(1 - \frac{\Delta t}{|T|}\left(\mu_i^p\right)^+\right)\varphi_l^1(M_i) - \frac{\Delta t}{|T|}\left(\mu_i^p\right)^+\lambda_l^-\varphi_l^1(M_1)\right\}\mathbf{\Upsilon}_i^p(\mathbf{r}_l^1),$$

Since $\lambda_l^- \leq 0$ and $\left(\mu_i^p\right)^+ \geq 0$, *this shows the stability of the scheme under a CFL like condition,*

$$\forall i, \text{ and } p, \;\; \frac{\Delta t}{|T|}\left(\mu_i^p\right)^+ \leq 1 \tag{33}$$

4.2.4 Summary

In this section we have shown that within a triangle T, the piecewise linear interpolation of U_j can be decomposed as a sum of simple waves

$$U(\mathbf{x}) = \sum_\sigma \varphi_\sigma(\mathbf{x})\mathbf{r}_\sigma \tag{34}$$

where φ_σ is of the form

$$\varphi_\sigma(\mathbf{x}) = \alpha_\sigma\,(\vec{n}_\sigma, \mathbf{x})$$

with $\alpha \in \mathbb{R}$, $\vec{n}_\sigma$ is a vector of norm unity and $\mathbf{r}_\sigma$ is an eigenvector of $\mathbf{K}_{\vec{n}_\sigma}$.

The three schemes considered here are linear, so the residuals sent to node M_j is the sum of the residual sent to this node by $U_\sigma(\mathbf{x}) = \varphi_\sigma(\mathbf{x})\mathbf{r}_\sigma$, namely

$$\Phi_i = \sum_\sigma \Phi(U_\sigma(\mathbf{x}))_i$$

with some abuse of language.

The scheme can be written as

$$U_i^{n+1} = \sum_{T, M_i \in T} \frac{|T|}{3|C_i|}\widetilde{U}_i^{n+1} \tag{35}$$

with

$$\widetilde{U}_i^{n+1} = U_i^n - \frac{\Delta t}{3|T|}\Phi_i. \tag{36}$$

We have shown that the three schemes under consideration satisfy, for any simple wave U_σ, the updated

$$\widetilde{U}_i = U_\sigma(M_i) - \frac{\Delta t}{3|T|}\Phi_i(U_\sigma)$$

satisfies

$$||\widetilde{U}_i|| \leq \max_{M_j \in T}||U_\sigma(M_j)|| \tag{37}$$

under a CFL type condition.

Gathering the properties and relations (34), (35), (36) and (37), we will say that the scheme is stable and monotone. We are not able to exhibit any norm for which, and for any solution, a relation like

$$||U_i^n|| \leq C(U^0)$$

would be true under a CFL like condition. From [8, 9], the classical L^p norms are not suitable, maybe the less standard $L_{p,\alpha}$ norms of [9] for which the Cauchy problem is well posed. From an experimental point of view, the conditions (34), (35), (36) and (37) seem sufficient ; this is why we call this stability.

4.3 Construction of LP schemes for systems

We present now a method for which, starting from the stable monotone scheme, enable the construction of monotone second order schemes at steady state. These LP schemes have a residual that write

$$\mathbf{\Phi}_i = \mathbf{B}_i \mathbf{\Phi}, \ \mathbf{B}_i \text{ matrix}$$

and are oscillation free. We show that they also satisfy the stability requirement decribed in section 4.2.4

4.3.1 Construction

The idea of the construction is the following. In each triangle T, if we can determine basis $(\mathbf{t}_l)_l$ such that

$$\begin{aligned}\mathbf{\Phi}_i &= \sum_l \varphi_i^l \mathbf{t}_l \\ \text{and } \mathbf{\Phi}_i &= \sum_{j,l} c_{ij}^l \left(\varphi_j^l - \varphi_i^l\right) \mathbf{t}_l\end{aligned} \tag{38}$$

with $c_{ij}^l \geq 0$, we have a scheme that preserves monotonicity in the meaning we have given this word in §4.2. This is the case of the Rusanov', the finite volume and the N schemes. This is a geometrical property of these schemes : it states that simple waves evolve in a non oscillatory manner. If now the simple wave is described in a basis for which (38) is not true, the property of generating oscillation free solution is a geometrical property of these schemes and should be true whatever the basis $(\mathbf{t}_l)_l$ chosen to represent the scheme. We justify this claim in §4.3.2. In particular

$$\mathbf{\Phi}_i = \sum_l \big((\mathbf{\Phi}_i, \mathbf{t}_l) \big) \mathbf{t}_l \tag{39}$$

we can rewrite the relations (38) with (39)

The idea is to choose a basis, to write (39), to notice that

$$\sum_j (\mathbf{\Phi}_j, \mathbf{t}_l) = (\mathbf{\Phi}, \mathbf{t}_l)$$

and to interpret the coefficients $(\mathbf{\Phi}_j, \mathbf{t}_l)$ as scalar residuals to which we apply the limitation technique of section 3. We construct residuals $\varphi_{l,i}^*$ such that

$$\begin{aligned}\sum_i \varphi_{l,i}^* &= (\mathbf{\Phi}, \mathbf{t}_l) \\ \varphi_{l,i}^* &= \beta_i^l (\mathbf{\Phi}, \mathbf{t}_l)\end{aligned} \tag{40}$$

with β_i^l bounded. The residual

$$\mathbf{\Phi}_i^* = \sum_l \varphi_{l,i}^* \mathbf{t}_l \tag{41}$$

can be rewritten as

$$\mathbf{\Phi}_i^* = \mathbf{B}_i \mathbf{\Phi} \tag{42}$$

where the matrix $\mathbf{B}_i$ is uniformly bounded by construction. In the next section, we show the scheme preserves the monotonicity.

4.3.2 Analysis

Consider an orthonormal basis $(\mathbf{t}_l)_l$. We construct the limited scheme by

$$\Phi_i^* = \mathbf{B}_i \Phi$$

that is

$$\Phi_i^* = \sum_\sigma \mathbf{B}_i \Phi(\varphi_\sigma(x)\mathbf{r}_\sigma).$$

The matrix $\mathbf{B}_i$ is constructed by

$$(\Phi_i^*, \mathbf{t}_l) = \mu_l\,(\Phi, \mathbf{t}_l)$$

with $\mu_l \in [0,1]$.

We set $\lambda = \dfrac{\Delta t}{3|T|}$. We have

$$\big|\big|U_i^n - \lambda \Phi_i\big|\big| = \sum_l \big(\,(U_i^n, \mathbf{t}_l) - \lambda \mu_l\,(\Phi, \mathbf{t}_l)\,\big)^2. \tag{43}$$

We want to show that under $\mu_l \in [0,1]$, (43) implies, for simple waves,

$$\big|\big|U_i^n - \lambda \Phi_i\big|\big| \leq \max_{M_j \in T} \big|\varphi_\sigma(M_j)\big|. \tag{44}$$

For a simple wave, we have

$$\Big(\,\Big(\widetilde{U}_i^{n+1}, \mathbf{t}_l\Big)\,\Big)^2 = \big(\varphi_\sigma\,(r_\sigma, \mathbf{t}_l) - \mu_l \lambda\,(\Phi_i, \mathbf{t}_l)\,\big)^2$$

which is convex in μ_i, so

$$\big(\varphi_\sigma\,(r_\sigma, \mathbf{t}_l) - \mu_l \lambda\,(\Phi_i, \mathbf{t}_l)\,\big)^2 \leq \max\Big(\big(\varphi_\sigma\,(r_\sigma, \mathbf{t}_l)\,\big)^2, \big(\varphi_\sigma\,(r_\sigma, \mathbf{t}_l) - \lambda\,(\Phi_i, \mathbf{t}_l)\,\big)^2\Big).$$

Hence, we can rewrite

$$\sum_l \Big(\,\Big(\widetilde{U}_i^{n+1}, \mathbf{t}_l\Big)\,\Big)^2 = \big|\big|\mathbf{P} U_i^n\big|\big|^2 + \big|\big|\mathbf{Q}\big(U_i^n - \lambda\Phi_i\big)\big|\big|^2$$

where $\mathbf{P}$ (resp. $\mathbf{Q}$) is the orthogonal projector onto the subspace generated by the vectors of $\{\mathbf{t}_l\}$ for which

$$\max\Big(\big(\varphi_\sigma\,(r_\sigma, \mathbf{t}_l)\,\big)^2, \big(\varphi_\sigma\,(r_\sigma, \mathbf{t}_l) - \lambda\,(\Phi_i, \mathbf{t}_l)\,\big)^2\Big) = \big(\varphi_\sigma\,(r_\sigma, \mathbf{t}_l)\,\big)^2$$

(resp.

$$\max\Big(\big(\varphi_\sigma\,(r_\sigma, \mathbf{t}_l)\,\big)^2, \big(\varphi_\sigma\,(r_\sigma, \mathbf{t}_l) - \lambda\,(\Phi_i, \mathbf{t}_l)\,\big)^2\Big) = \big(\varphi_\sigma\,(r_\sigma, \mathbf{t}_l) - \lambda\,(\Phi_i, \mathbf{t}_l)\,\big)^2 \qquad).$$

We consider the examples of the Rusanov scheme and the system N scheme for which we have shown that (44) is true.

Case of the Rusanov scheme. For a simple wave, we have shown that $\widetilde{U}_i^{n+1}$ is proportional to $\mathbf{r}$, and

$$\big|\big|\widetilde{U}_i^{n+1}\big|\big| \leq \max_{M_j \in T} \big|\varphi_\sigma(M_j)\big|$$

so $\mathbf{Q}\big(U_i^n - \lambda\Phi_i\big)$ is proportional to $\mathbf{Q}\big(\mathbf{r}\big)$ and we have

$$\begin{aligned}
\Big|\Big|\mathbf{P} U_i^n\Big|\Big|^2 + \Big|\Big|\mathbf{Q}\big(U_i^n - \lambda\Phi_i\big)\Big|\Big|^2 &\leq |\varphi_\sigma(M_i)|^2 \big|\big|\mathbf{Pr}\big|\big|^2 + \max_{M_j \in T} \big|\varphi_\sigma(M_j)\big|^2 \big|\big|\mathbf{Qr}\big|\big|^2 \\
&\leq \max_{M_j \in T} \big|\varphi_\sigma(M_j)\big|^2 \Big(||\mathbf{Pr}||^2 + ||\mathbf{Qr}||^2\Big) \\
&= \max_{M_j \in T} \big|\varphi_\sigma(M_j)\big|^2
\end{aligned}$$

because $\mathbf{P}$ and $\mathbf{Q}$ are two orthogonal projectors. This ends the proof in the case of the Rusanov' scheme.

Case of the system N scheme. For the sake of simplicity, we only consider the 2×2 case of the Cauchy–Riemann system. The proof is similar in the general case using the arguments of §4.2.3.

The Cauchy-Riemann system reads

$$\frac{\partial U}{\partial t}+\begin{pmatrix}-1 & 0\\ 0 & 1\end{pmatrix}\frac{\partial U}{\partial x}+\begin{pmatrix}0 & 1\\ 1 & 0\end{pmatrix}\frac{\partial U}{\partial y}=0.$$

Considering a direction $\vec{n}_i$, the eigenvalues of $K_i=K_{\vec{n}_i}$ are $\pm||\vec{n}_i||$, and the normalised orthogonal eigenvectors are denoted by $\mathbf{r}_i^{\pm}$. An easy calculation shows that $\big|\big|K_i\big|\big|=\big|\big|\vec{n}_i\big|\big|\mathbf{Id}$ hence,

$$\sum_{i=1}^{3}K_i^- = -\frac{2}{\sum\limits_{j=1}^{3}||\vec{n}_i||}\mathbf{Id} := \alpha\mathbf{Id}.$$

Using this remark, we see that for a general simple wave $U_i=\varphi_\sigma(M_i)\mathbf{r}$, we have

$$\widetilde{U}=N\big(\sum_{j=1}^{3}K_j^-U_j\big)=\alpha\big(\sum_{j=1}^{3}||\vec{n}_j||\varphi_\sigma(M_j)\big(\,\big(\mathbf{r},\mathbf{r}_i^-\big)\,\big)^2\big)\mathbf{r},$$

and then, with $c_{ij}=\alpha||\vec{n}_j||\;||\vec{n}_i||\left(\mathbf{r},\mathbf{r}_i^-\right)^2\geq 0$,

$$\widetilde{U}_i^{n+1}=U_i^n-\lambda\sum_{j=1}^{3}c_{ij}\left(\varphi_\sigma(M_i)-\varphi_\sigma(M_j)\right)\big(\,\left(\mathbf{r}_i^+,\mathbf{r}\right)\,\big)\mathbf{r}_i^+$$

because (setting $\varphi_\sigma(M_j)\equiv 1$), $\alpha\big(\sum\limits_{j=1}^{3}||\vec{n}_j||\big(\,\left(\mathbf{r},\mathbf{r}_i^-\right)\,\big)^2\big)=1$.

Another way of stating this result is

$$\begin{aligned}
&\left(\widetilde{U}_i^{n+1},\mathbf{r}_i^+\right)=\left\{\varphi_\sigma(M_i)-\lambda\left(\sum_{j=1}^{3}c_{ij}\big(\varphi_\sigma(M_i)-\varphi_\sigma(M_j)\big)\right)\right\}\big(\,\left(\mathbf{r},\mathbf{r}_i^+\right)\,\big):=\mathcal{A}\,\left[\,\left(\mathbf{r},\mathbf{r}_i^+\right)\,\right]\\
&\left(\widetilde{U}_i^{n+1},\mathbf{r}_i^-\right)=\varphi_\sigma(M_i)\big[\,\left(\mathbf{r},\mathbf{r}_i^-\right)\,\big]
\end{aligned}$$

We have

$$\begin{aligned}
\big|\big|\mathbf{Q}\big(\widetilde{U}_i^{n+1}\big)\big|\big|^2 &= \big|\big|\mathbf{Q}\big(\mathcal{A}\big[\,\left(\mathbf{r},\mathbf{r}_i^+\right)\,\big]\mathbf{r}_i^+\big)\big|\big|^2+\big|\big|\mathbf{Q}\big(\varphi_\sigma(M_i)\big[\,\left(\mathbf{r},\mathbf{r}_i^-\right)\,\big]\mathbf{r}_i^-\big)\big|\big|^2\\
&\leq \max_{M_j\in T}\big|\varphi_\sigma(M_j)\big|^2\left\{\big|\big|\mathbf{Q}\big(\,\left(\mathbf{r},\mathbf{r}_i^+\right)\,\mathbf{r}_i^+\big)\big|\big|^2+\big|\big|\mathbf{Q}\big(\big[\,\left(\mathbf{r},\mathbf{r}_i^-\right)\,\big]\mathbf{r}_i^-\big)\big|\big|^2\right\}\\
&= \max_{M_j\in T}\big|\varphi_\sigma(M_j)\big|^2\;\big|\big|\mathbf{Q}\big(\mathbf{r}\big)\big|\big|^2
\end{aligned}$$

because $\mathbf{Q}$ is an orthogonal projector. Then, since $\mathbf{P}$ and $\mathbf{Q}$ are orthogonal projectors, we have

$$\big|\big|\mathbf{P}\big(\mathbf{r}\big)\big|\big|^2+\big|\big|\mathbf{Q}\big(\mathbf{r}\big)\big|\big|^2=1$$

so

$$\big|\widetilde{U}_i^{n+1}\big|^2\leq\max_{M_j\in T}\big|\varphi_\sigma(M_j)\big|^2$$

because

$$\mathcal{A}^2\leq\max_{M_j\in T}\big|\varphi_\sigma(M_j)\big|^2.$$

4.4 Example of the Cauchy–Riemann equations

We consider the Riemann problem

$$\begin{gathered}\frac{\partial U}{\partial t}+A\frac{\partial U}{\partial x}+B\frac{\partial U}{\partial y}=0 \qquad t>0\\ \text{Riemann data per quadrangle}\end{gathered} \tag{45}$$

The matrices A and B are

$$A=\begin{pmatrix}1 & 0\\ 0 & -1\end{pmatrix} \text{ et } B=\begin{pmatrix}0 & 1\\ 1 & 0\end{pmatrix}.$$

We test the scheme of §4.3 on the following Riemann data $U=(u,v)$

$$u=\begin{cases}1 & \text{if } x>0 \text{ and } y>0\\ -1 & \text{if } x<0 \text{ and } y>0\\ -1 & \text{if } x>0 \text{ and } y<0\\ 1 & \text{if } x<0 \text{ and } y<0\end{cases} \text{ and } v=\begin{cases}1 & \text{if } x>0 \text{ and } y>0\\ -1 & \text{if } x<0 \text{ and } y>0\\ -1 & \text{if } x>0 \text{ and } y<0\\ 2 & \text{if } x<0 \text{ and } y<0\end{cases} \tag{46}$$

The solution is self similar, $U(x,y,t)=\widetilde{U}(\frac{x}{t},\frac{y}{t})$. The function $\widetilde{U}$ satisfies

$$\xi\frac{\partial U}{\partial \xi}-\nu\frac{\partial U}{\partial \nu}+A\frac{\partial U}{\partial \xi}+B\frac{\partial U}{\partial \nu}=0 \tag{47}$$

with the boundary conditions at infinity given by the Riemann data (45–46) at time $t=1$. The problem is solved by a time marching technique. The computational domain is $[-2,2]\times[-2,2]$. The solution of (47) corresponds to the solution of the Riemann problem (46) The PDE (47) is elliptic in $\xi^2+\nu^2\leq 1$ and hyperbolic in $\xi^2+\nu^2\geq 1$.

In the method, the choice of the orthogonal basis is free. In $\mathbb{R}^2$, they can be indexed by the angle θ. We have chosen here the eigenvectors of $\cos\theta A+\sin\theta B$. The results are presented for the limited N scheme.

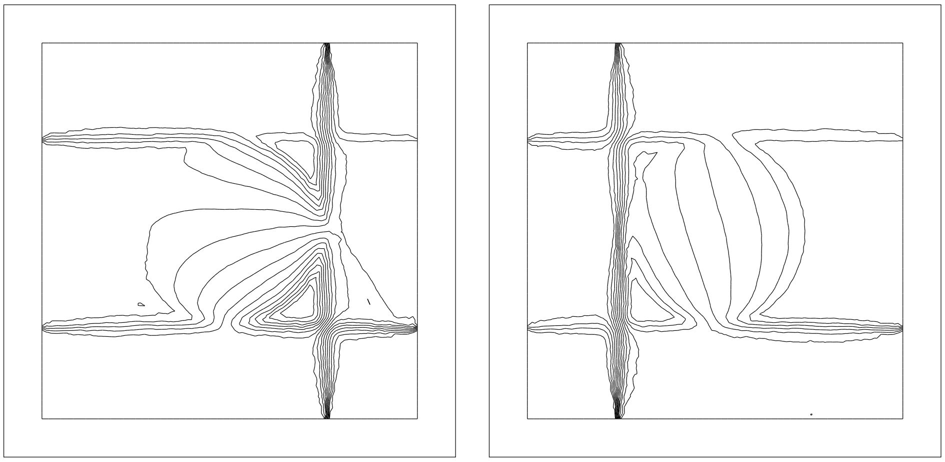

Figure 10: Solutions (right : u, left : v) for the N scheme.

We see that the limited solutions are much more accurate than the first order scheme. The quality of the solution does not depend on the angle, as conjectured. The choice $\theta=\arctan\left(\frac{u}{v}\right)$ corresponds to the dot multiplication of (45) by $(u,v)^T$. This means that we wish to control the entropy production of the scheme, since it is given by

$$(u,v)^T\frac{\partial}{\partial t}\begin{pmatrix}u\\ v\end{pmatrix}=-uA\frac{\partial U}{\partial x}-vB\frac{\partial U}{\partial y}.$$

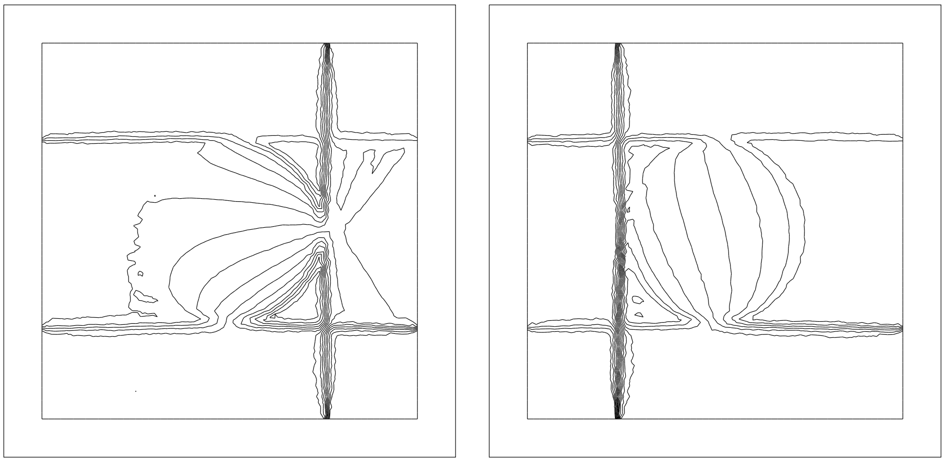

Figure 11: Solutions (right : u, left : v) for the limited N scheme, $\theta = 0°$

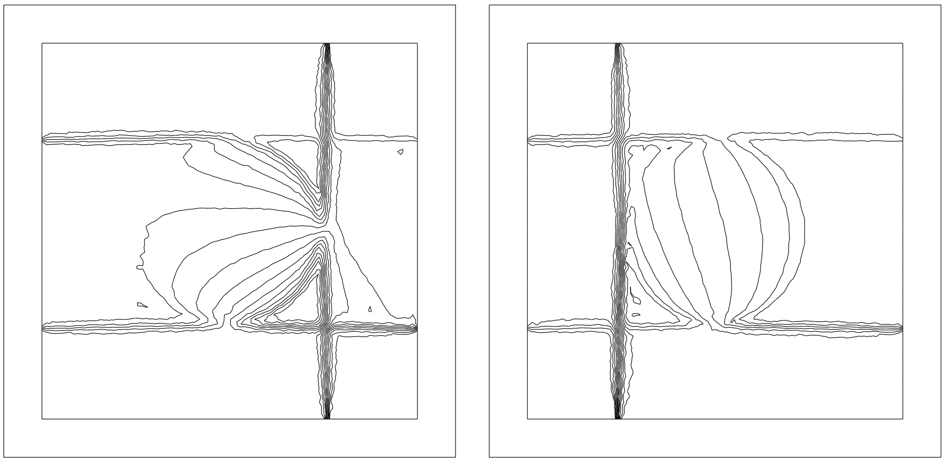

Figure 12: Solutions (right : u, left : v) for the limited N scheme, $\theta = 45°$

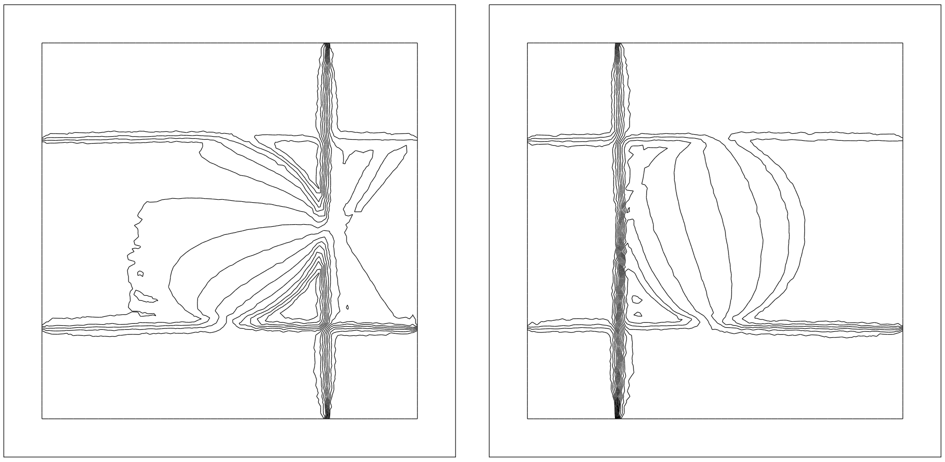

Figure 13: Solutions (right : u, left : v) for the limited N scheme $\theta = \arctan\left(\frac{u}{v}\right)$

5 Case of the Euler equations

First, as in [10], the non linear problem is replaced by a linearised one in each triangle. It is well known that the state vector and the Euler fluxes are quadratic in

$$Z = \sqrt{\rho}(1, \mathbf{u}, H)^T$$

where H is the enthalpy of the fluid. For example, we have $W = \frac{1}{2}D(Z)Z$ where $D(Z)$ is linear in Z. For this to be true, one needs that the ratio of specific heats γ be constant. This is what we assume.

Thanks to the linearisation, the problem reduces to

$$\frac{\partial W}{\partial t} + \bar{A}\frac{\partial Z}{\partial x} + \bar{B}\frac{\partial Z}{\partial y} = 0$$

where the Jacobians $\bar{A}$ and $\bar{B}$ are functions of the average of Z on T, [10]. Once this is done, we consider the N scheme and the limited scheme as described in §4.3. For example the N scheme writes

$$|C_i|\frac{W_i^{n+1} - W_i^n}{\Delta t} + \sum_{T, M_i \in T} \Phi_i^T = 0$$
$$\Phi_i^T = \sum_{M_j \in T} K_i^+ N K_j^- \left(\widetilde{W}_i^n - \widetilde{W}_j^n\right).$$

Here, $\widetilde{W} = \frac{1}{2}D(\bar{Z})Z$, and K_i is evaluated at the state $\bar{W} = \frac{1}{2}D(Z)\bar{Z}$.

In the simulations, we consider two types of boundary conditions : wall and inflow/outflow conditions. They are approximated as in [3]. More precisely, the inflow/outflow conditions are got thanks to Steger–Warming flux modified as in [13], and written in fluctuation form. The wall condition reduces to imposing weakly a no slip condition. Here, as in [13], we have chosen to impose the flux

$$\mathcal{F} = \begin{pmatrix} 0 \\ pn_x \\ pn_y \\ 0 \end{pmatrix}$$

written in fluctuation form. Other solutions are possible, such as the ones described in Paillère's thesis [23].

The limited N scheme has been tested against numerous test cases in subsonic, transonic and supersonic situations. We only present the most significant examples.

We have also tested the same technique where the monotone first order scheme is now defined by the standard Roe scheme [26] written in fluctuation form. We obtain a second order scheme, as in the standard high order scheme, but here the stencil is as compact as for the first order scheme, in contrast with what is done usually. The extension is done formaly.

In each problem, the initial condition is a uniform flow given by the conditions at infinity. The scheme is implicit, the implicit phase is provided by an approximate linearisation of the first order Roe solver. Our aim is not to have a maximum efficiency, but to show the accuracy of the new scheme, as well as the robustness of the method.

5.1 Flow around a NACA 0012, $\mathcal{M}_\infty = 0.85$, $\theta = 1°$

The mesh is plotted on Figure 14. We plot the velocity for the N scheme and the limited N scheme, Figure 15. This shows the improvement of the slip line at the leading edge of the airfoil. We also present the pressure isoline on Figure 16. The pressure coefficient along the airfoil is provided on Figure 17. The Figure 18 presents the entropy deviation ; there is a clear improvement. On Figure 17, we compare the pressure coefficient obtained by the scheme of [3] and the present one. We see that the new scheme provides oscillation free solutions, where as the blending of the N and LDA scheme [4] of [3] was providing slight oscillations. The comparison of the entropy deviation between the new scheme and the blended scheme of [3], we also see a clear improvement.

[4]The LDA scheme is defined by $\Phi_i = -NK_i^+\Phi$.

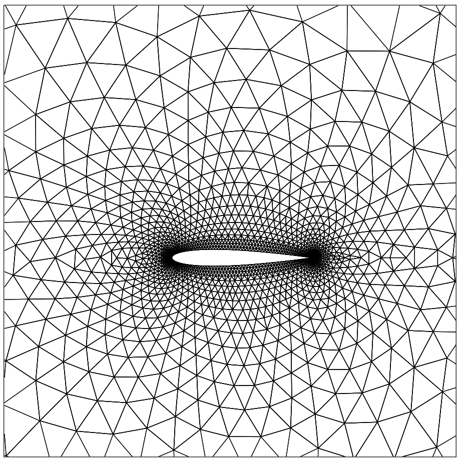

Figure 14: Zoom of the mesh

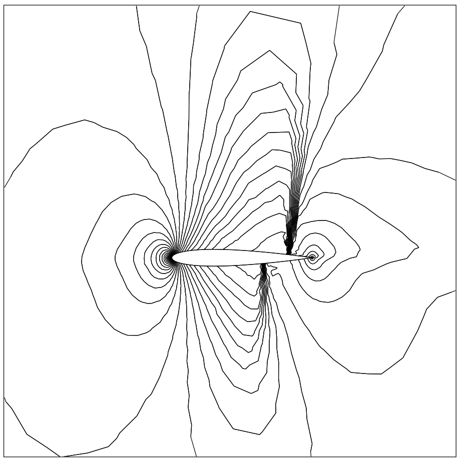

N scheme

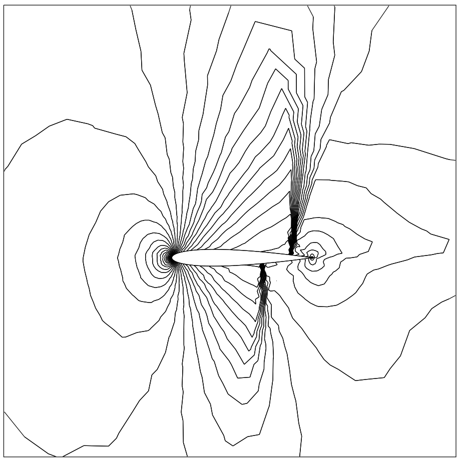

Limited scheme

Figure 15: Velocity isolines

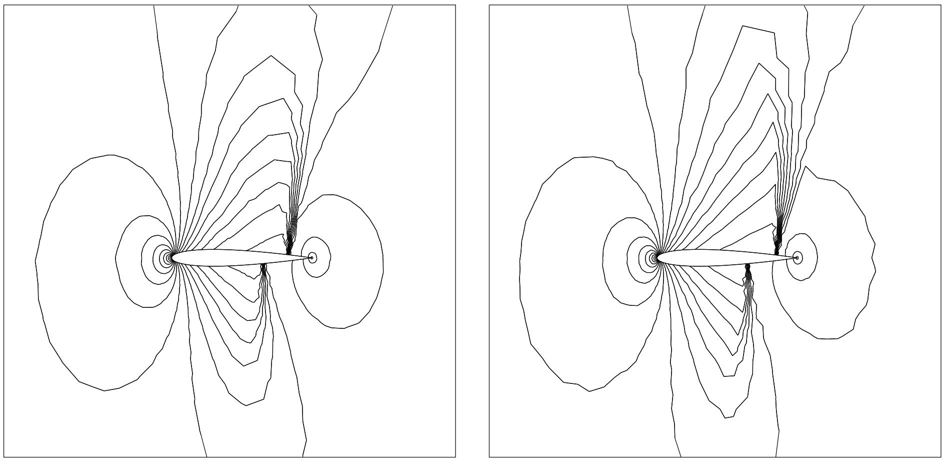

N scheme Limited scheme

Figure 16: Pressure isolines

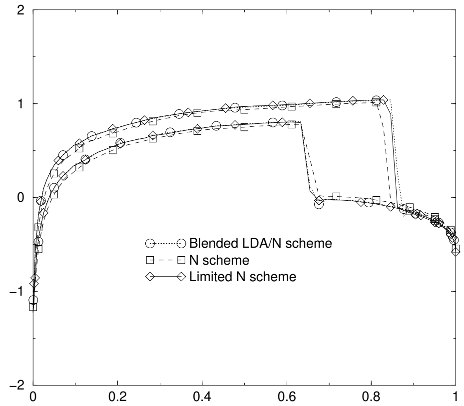

Figure 17: Plot of cp along the airfoil

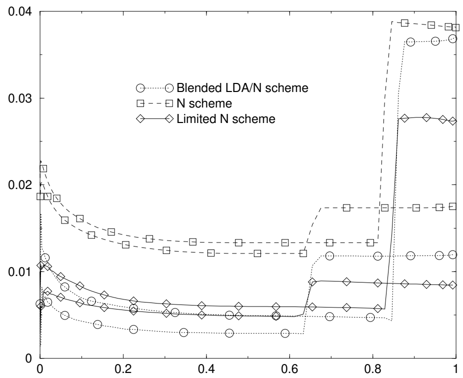

Figure 18: Entropy deviations along the airfoil

5.2 Hypersonic flow, $\mathcal{M}_\infty = 8$.

It was not possible to run this test case with the scheme of [3], because very quickly negative pressure problems were occuring. A zoom of the mesh is given on Figure 19. The mach number for the N scheme and the limited scheme are given on Figure 20. We also give cross–sections of the density (Fig. 22), of the Mach number (Fig. 21) and the entropy deviation (Fig. 23) along the symetry axis. Our results are clearly oscillation free. The boundary conditions are better taken into account with the limited scheme.

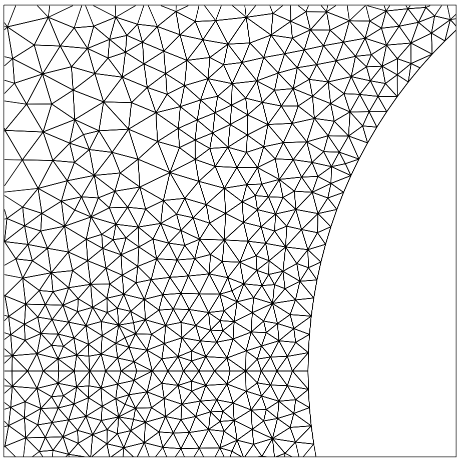

Figure 19: Mesh

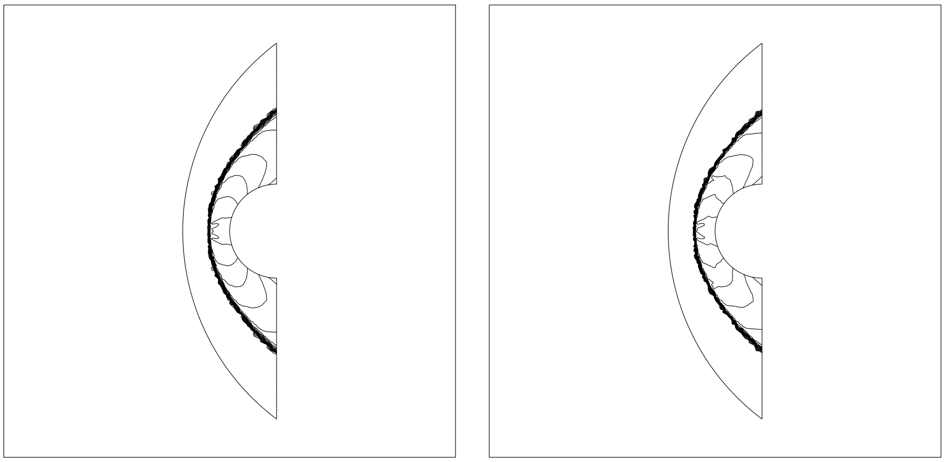

N scheme

Limited scheme

Figure 20: Isomach lines, limited N scheme

5.3 Subsonic cylinder, $\mathcal{M}_\infty = 0.35$

We have run this subsonic test case with the N scheme, the Limited N scheme, the LDA scheme and the blended N/LDA scheme of [7]. We display the Mach number on Figure 24 and the entropy deviation on Figure 25. In both case, we have plotted the same isolines. The mesh is similar as in Figure 19. As expected the best results are obtained with the LDA scheme. This is particularly clear from the entropy deviation and mach number isolines. The mach isolines are symetric with respect to the axis orthogonal to the velocity

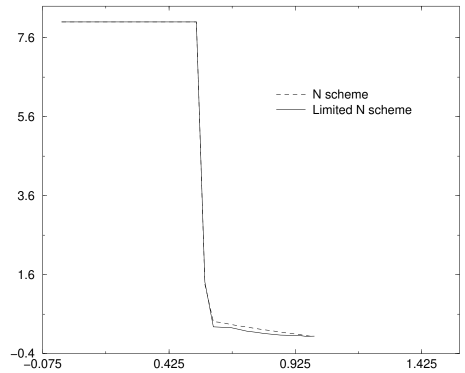

Figure 21: Cross–section of the Mach number

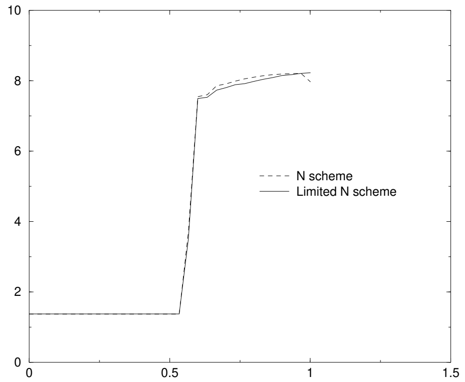

Figure 22: Cross–section of the density

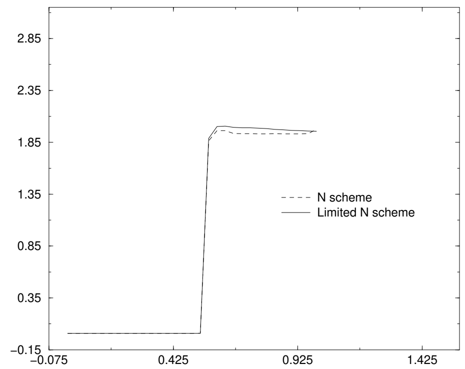

Figure 23: Cross–section of the entropy deviation

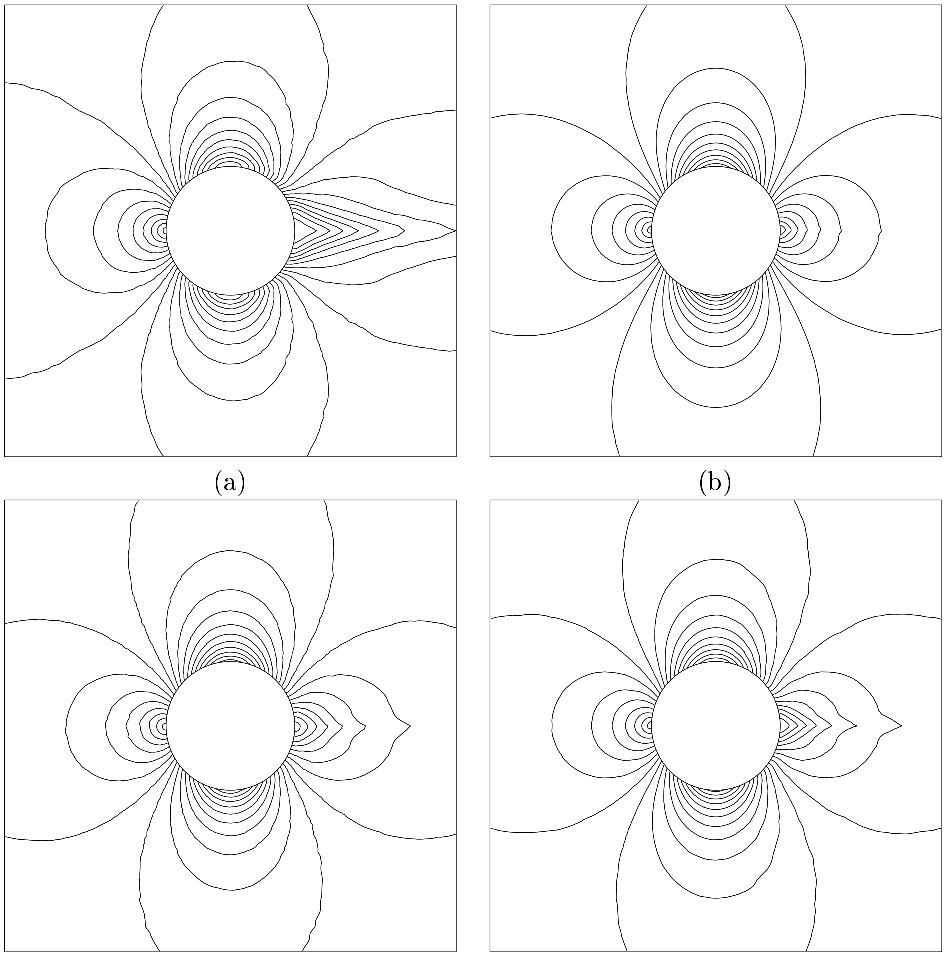

(a) (b) (c) (d)

Figure 24: Mach number isolines (a) : N scheme (min=0, max=0.756), (b) : LDA scheme (min=0.001, max=0.84), (c) : Limited N scheme (min=0.002, max=0.83), (d) Blended LDA/N scheme (min=0.002, max=0.82)

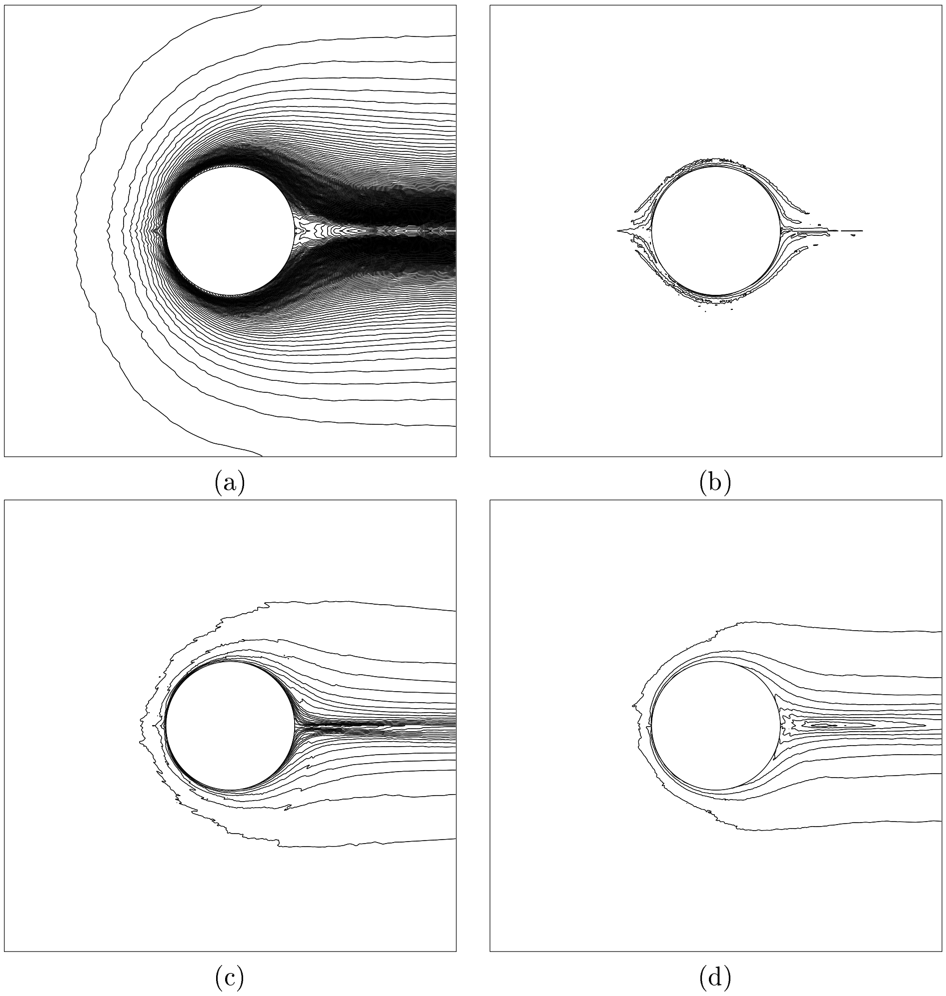

Figure 25: Entropy deviation isolines (a) : N scheme (min=0, max=0.007), (b) : LDA scheme (min=-0.0002, max=0.0002), (c) : Limited N scheme (min=0, max=0.0014), (d) Blended LDA/N scheme (min=0, max=0.0007)

at infinity, as it should be. As expected, the worst results are obtained for the N scheme. The results for the Limited N and Blended scheme are of similar quality. The entropy deviation is better for the Blended LDA/N scheme, but the approximated symetry of the mach number isolines is better respected with the Limited N scheme.

5.4 Scramjet

We have run the N scheme, the LDA scheme, the blended scheme of [7], Deconinck et al. B scheme [11] and the Limited N scheme on a scramjet–like case. Our implementation of the B scheme is the follwoing. We first compute the N and LDA residuals denoted respectively Φ_i^N and Φ_i^{LDA} for $i = 1, \cdots, 3$. Then we consider the right and left eigenvectors associated to the flow direction (the result is rather independant of the choice, and qualitatively independant of this choice). We denote them by $\mathbf{r}_l$ and ℓ_l, $l = 1, 4$. Then we compute $\ell_l(\Phi_i^N)$ and $\ell_l(\Phi_i^{LDA}$. Next we introduce the blending parameters μ_l, $l = 1, \cdots, 4$,

$$\mu_l = \frac{\left|\sum\limits_{i=1}^{3} \ell_l(\Phi_i^N)\right|}{\sum\limits_{i=1}^{3} \left|\ell_l(\Phi_i^N)\right| + \epsilon}, \qquad \epsilon = 10^{-10}.$$

Then the B scheme writes

$$\Phi_i^B = \sum_{l=1}^{4} \Big(\ell_l(\Phi_i^{LDA}) + \mu_l \big(\ell_l(\Phi_i^N) - \ell_l(\Phi_i^{LDA}) \big) \Big) \mathbf{r}_l.$$

The geometry has been found on `http:://www.inria.fr/`, the mach number at infinity is set to 3.5. A zoom of the mesh is given on Figure 26. This case is interesting because it provides a good example

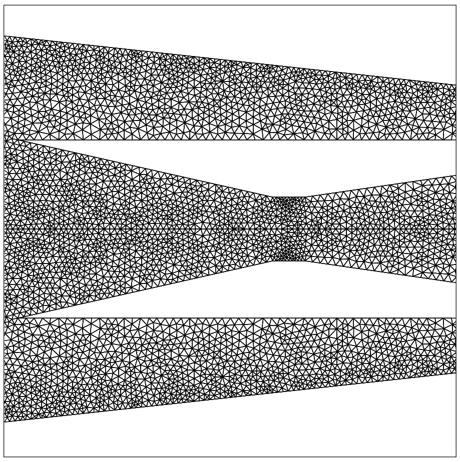

Figure 26: Zoom of the mesh for the scramjet case

of the difference between the schemes. The Mach number is displayed on Figure 27. We have used the same isolines. The most dissipative is once more the N scheme. The least dissipative is the LDA scheme, but it is very oscillatory. The three other schemes are monotone. The blended scheme of [7] is the most dissipative among the three (this is clear from the structure of the reflected shocks). The B scheme has a better behaviour with respect to this criterion, but the best is the Limited N scheme. This is coufirmed by the Mach number distribution on the line $y = 0.3$ in the throat, see Figure 28.

This shows that the choice of the blending parameters is important (the B scheme has a richer structure than the scheme of [7]), but the construction presented in this paper seems the most efficient.

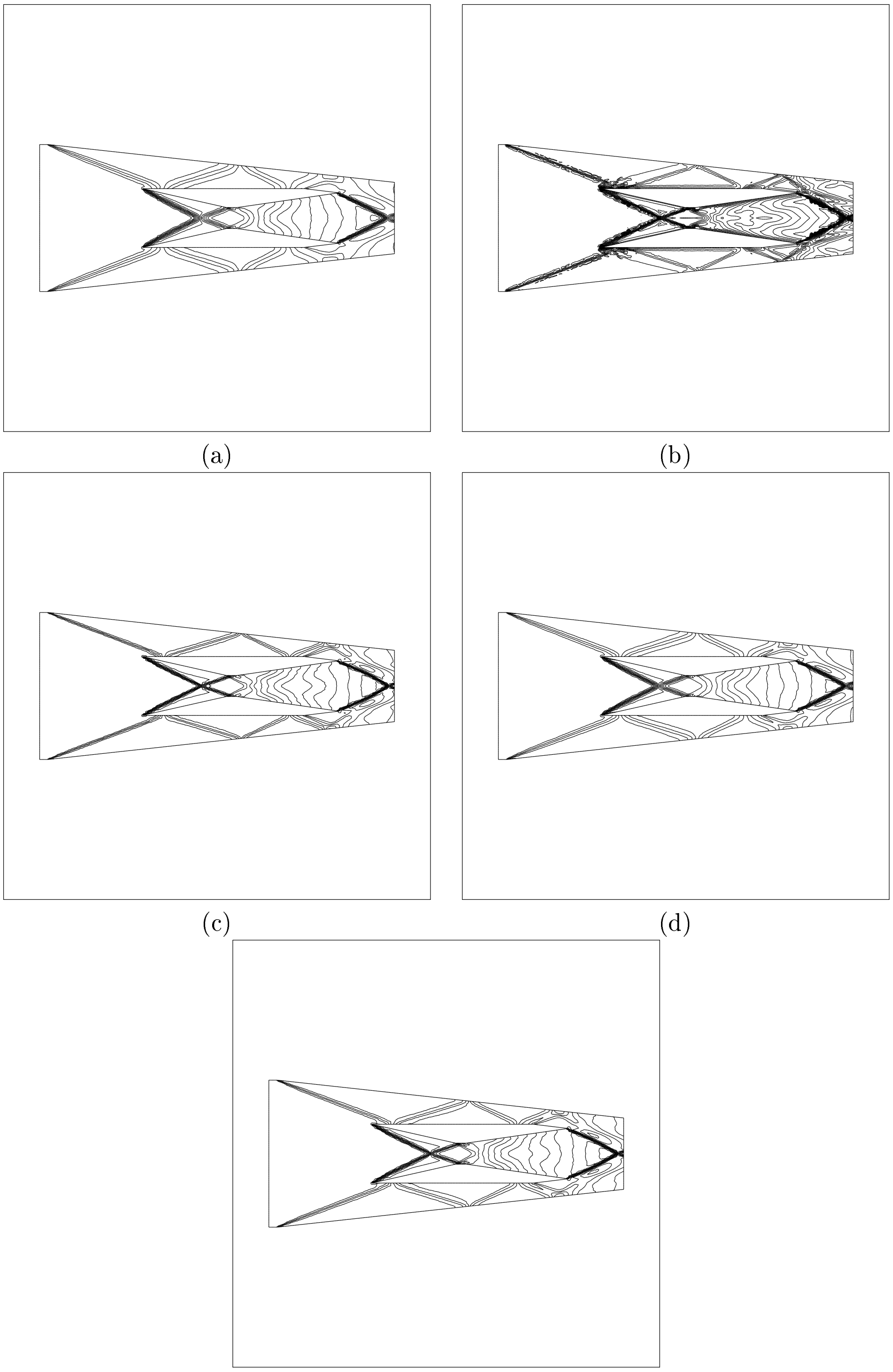

(a) (b)

(c) (d)

(e)

Figure 27: Mach number isolines (a) : N scheme (min=1.97, max=3.6), (b) : LDA scheme (min=1.44, max=6.47), (c) : Limited N scheme (min=1.85, max=3.6), (d) Blended LDA/N scheme (min=1.87, max=3.6), (e) B scheme (min=1.88, max=3.6)

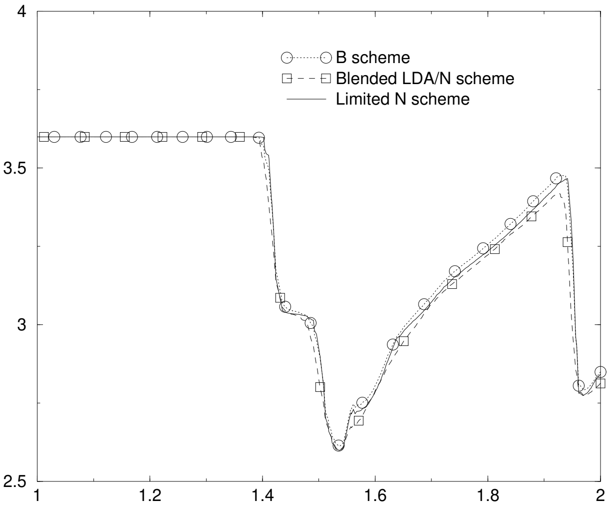

Figure 28: Mach number distribution along $y = 0.3$ in the throat

6 Conclusions

We have presented and analysed a stable and monotone method for the computation of compressible flows. The schemes we develop are formaly second order accurate on regular unstructured meshes. The capabilities of the schemes are presented on several subsonic, transonic and supersonic flows. The results are good. Compared with any scheme constructed by blending two schemes, as in [3] or [11], the computational complexity is reduced by a half, since only a first order scheme has to be evaluated.

We have used very crude boundary conditions in this paper, in particular the wall b.c. could be improved along the lines of Paillère's thesis, where it become easy to incorporate the limitation technique developped in the paper. This is done in [7].

The main problem is in the non–linear convergence history. The scalar results are converged : the L^2 residual of our results is below 10^{-7}. Going to system, the situation is much less clear. We have been able to drop the L^2 and L^∞ residual for the Cauchy–Riemann problem below 10^{-7}, but the convergence history depends very much on the mesh, and on the angle θ in §4.4. In particular the convergence history is much smoother when θ is the same throughout the mesh. In some other tests, we were not able to drop the residual below 10^{-3}. In the Euler case, except for very coarse meshes, we were never able to drop the residual below 10^{-3}. However, in each case, most of the mesh points are converged, only very few of them have an erratic convergence history. The reason of this behavior are not understood.

Last, an extension of these methods to unsteady flow fields is presented in [7].

Acknowledgements

This work has been performed under a CEA grant through the "Laboratoire correspondant du Cea" LRC-03. The first author also acknowledge the hopitality of RIACS, NASA Ames Researc Center, where part of this work has been performed.

References

[1] R. Abgrall, *A genuinely multidimensional Riemann solver*, Tech. Rep. 1859, INRIA, Février 1993.

[2] ——, *On Essentially Non-Oscillatory Schemes on Unstructured Meshes : Analysis and Implementation*, J. Comp. Phys., 114 (1994), pp. 45–54.

[3] ——, *Toward the ultimate conservative scheme : Following the quest*, J. Comput. Phys., (accepted for publication).

[4] R. Abgrall and T. Barth, *Weighted residual distribution schemes for conservation laws via adaptive quadrature*, Siam J. Sci. Comput., (en révision, 2001).

[5] R. Abgrall, S. Lantéri, and T. Sonar, *Eno schemes for compressible fluid dynamics*, ZAMM, 79 (1999), pp. 3–28. Rapport de l'Institut fur Mathematik der Universitaet Hamburg, num 116, Decembre 1996.

[6] R. Abgrall, K. Mer, and B. Nkonga, *A lax–wendroff type theorem for residual schemes*, in Proceeding of a conference for P.L. Roe's 60th birthsday, M. Hafez and J. Chattot, eds., Wiley, to appear.

[7] R. Abgrall and M. Mezine, *Construction of second order accurate monotone and stable residual schemes : the unsteady case*, tech. rep., MAB, 2001.

[8] P. Brenner, *The cauchy problem for symmetric hyperbolic systems in l^p*, Math. Scan., 19 (1966), pp. 23–27.

[9] ——, *The cauchy problem for systems in l_p and l_p, α*, Ark. Mat., 11 (1973), pp. 75–101.

[10] H. Deconinck, P. Roe, and R. Struijs, *A multidimensional generalisation of Roe's difference splitter for the Euler equations*, Computer and Fluids, 22 (1993), pp. 215–222.

[11] H. Deconinck, K. Sermeus, and R. Abgrall, *Status of multidimensional upwind residual distribution schemes and applications in aeronautics.* AIAA paper 2000-2328, June 2000. AIAA CFD Conference, Denver (USA).

[12] H. Deconinck, R. Struijs, G. Bourgeois, and P. Roe, *Compact advection schemes on unstructured meshes.* VKI Lecture Series 1993–04, Computational Fluid Dynamics, 1993.

[13] L. Fezoui and B. Stoufflet, *A class of implicit upwind schemes for Euler simulations with unstructured meshes*, J. Comput. Phys., 84 (1989), pp. 174–206.

[14] O. Friedrich, *Weighted essentially non-oscillatory schemes for the interpolation of mean values on unstructured grids.*, J. Comput. Phys., 144 (1998), pp. 194–212.

[15] H. Gilquin, J. Laurens, and C. Rosier, *Multi-dimensional riemann problems for linear hyperbolic systems*, RAIRO, Modelisation Math. Anal. Numer, 30 (1996), pp. 527–548.

[16] E. Godlewski and P. Raviart, *Hyperbolic systems of conservations laws, I*, Ellipse, 1991.

[17] ——, *Hyperbolic systems of conservations laws*, Applied Mathematical Sciences, Springer Verlag, 1995.

[18] A. harten and S. Chakravarthy, *Multidimensional eno schemes for general geometries*, tech. rep., ICASE, 1991.

[19] C. Hu and C. Shu, *Weighted essentially non-oscillatory schemes on triangular meshes.*, J. Comput. Phys., 150 (1999), pp. 97–127.

[20] T. Hughes and M. Mallet, *A new finite element formulation for Computational Fluid Dynamics : IV a discontinuity–capturing operator for multidimensional advective–diffusive systems*, Computer Methods in Applied Mechanics and Engineering, 58 (1986), pp. 329–336.

[21] M. Hussaini, B. van Leer, and J. V. Rosendal, eds., *Upwind and High Resolution Schemes*, Springer Verlag, 1997.

[22] C. Johnson, U. Nävert, and J. Pitkäranta, *Finite element methods for linear hyperbolic problems*, Computer methods in applied mechanics and engineering, (1984), pp. 285–312.

[23] H. Paillère, *Multidimensional Upwind residual Discretisation Schemes for the Euler and Navier Stokes Equations on Unstructured Meshes*, PhD thesis, Université Libre de Bruxelles, 1995.

[24] P. Roe and D. Sidilkover, *Optimum positive linear schemes for advection in two and three dimensions.*, Siam J. Numer. Anal., 29 (1992), pp. 1542–1588.

[25] P. Roe and D. Sidlikover, *Optimum positive linear schemes for advection in two and three dimensions.*, SIAM J. Numer. Anal., 29 (1992), pp. 1542–1568.

[26] P. L. Roe, *Approximate Riemann solvers, parameter vectors, and difference schemes*, J. Comput. Phys., 43 (1983).

[27] R. Struijs, H. Deconinck, and P. L. Roe, *Fluctuation Splitting Schemes for the 2D Euler equations*, VKI LS 1991-01, Computational Fluid Dynamics, (1991).

[28] E. van der Weide, *Compressible Flow Simulation on Unstructured Grids using Multi-dimensional Upwind Schemes*, PhD thesis, Delft University of Technology, Netherlands, 1998.

[29] E. van der Weide and H. Deconinck, *Positive matrix distribution schemes for hyperbolic systems*, in Computational Fluid Dynamics '96, Wiley, 1996, pp. 747–753.

[30] B. van Leer, *Progress in multidimensional upwinding*, Tech. Rep. 92–43, ICASE, 1992.

[31] P. Vankeirsbilk and H. Deconinck, *Solution of the compressible euler equations with high order eno-schemes on general unstructured meshes*, in Computational Fluid Dynamics '92, Hirsch, Périaux, and Kordulla, eds., Elsevier, 1992, pp. 843–850.